AGU ADVANCING EARTH AND SPACE SCIENCES

JGR Atmospheres

RESEARCH ARTICLE
10.1029/2025JD043918

Key Points:

- A model with moisture-tagging capability is used to comprehensively attribute the moisture sources of Arctic atmospheric rivers (ARs)
- Arctic ARs draw moisture from both their genesis regions and transport pathways, with external sources surpassing local contributions
- Both local and external sources contribute to the observed cold season Arctic moistening, while external sources dominate in the warm season

Supporting Information:

Supporting Information may be found in the online version of this article.

Correspondence to:

W. Ma and H. Wang,
weiming.ma@pnnl.gov;
hailong.wang@pnnl.gov

Citation:

Ma, W., Wang, H., Zhang, S., Singh, B., Qian, Y., Huo, Y., et al. (2025). Quantifying moisture sources of Arctic atmospheric rivers during the recent historical period. *Journal of Geophysical Research: Atmospheres*, *130*, e2025JD043918. https://doi.org/10.1029/2025JD043918

Received 19 MAR 2025
Accepted 28 SEP 2025

Quantifying Moisture Sources of Arctic Atmospheric Rivers During the Recent Historical Period

Weiming Ma[1], Hailong Wang[1], Shixuan Zhang[1], Balwinder Singh[1], Yun Qian[1], Yiling Huo[1], Nicole Feldl[2], and Alexandre Audette[2]

[1]Atmospheric, Climate, and Earth Sciences Division, Pacific Northwest National Laboratory, Richland, WA, USA,
[2]Department of Earth and Planetary Sciences, University of California, Santa Cruz, Santa Cruz, CA, USA

Abstract Atmospheric rivers (ARs), filaments of intense atmospheric moisture transport, play a significant role in delivering moisture poleward into the Arctic and triggering weather extremes. Although previous studies have focused on large-scale circulations driving these events, this study investigates ARs through attributing their moisture sources using the Community Atmosphere Model version 5 (CAM5) with moisture-tagging capability. Examining ARs in the Atlantic and Pacific sectors of the Arctic separately revealed distinct contributions from remote versus local, and ocean versus land, moisture sources. Unlike non-AR events, Arctic ARs primarily draw moisture from their respective ocean basins in lower-latitude regions during the cold season, and shift to land sources in the warm season. Cold-season ARs in the Atlantic and Pacific sectors source 73.2% and 85.3% of their moisture from their respective ocean basins at lower latitudes, however warm-season contributions decrease to 41.3% and 29.4%. In contrast, mid- and high-latitude continents combined contribute 40.1% and 51.3% in the warm season. Trajectory clustering analysis shows that AR moisture sources depend on both their genesis regions and transport pathways. In recent decades, the Arctic has experienced a moistening trend in both the cold and warm seasons. Our results suggest that local and remote sources equally drive the observed cold-season moistening, whereas remote sources predominantly drive the warm-season moistening. A better understanding of Arctic AR moisture sources under current climate conditions provides valuable insights into their potential future changes amid the projected heterogeneous northern hemispheric warming.

Plain Language Summary Atmospheric rivers (ARs) are narrow bands of concentrated moisture that transport water vapor over long distances, playing a crucial role in the Arctic environment. Understanding where ARs source their moisture is essential for predicting their formation and variability. In this study, we used a climate model with advanced water-tracking capabilities to investigate the moisture sources for ARs entering the Arctic through the Atlantic and Pacific gateways. We find that Arctic ARs primarily draw their moisture from distant regions, with the specific source regions varying by season and transport pathway. During the cold season, Arctic ARs rely heavily on moisture from remote oceanic regions, such as the North Atlantic and North Pacific. In the warm season, they also tap into continental sources, particularly from mid- and high-latitude land surface regions. Additionally, we observed that the Arctic is becoming more humid in both the cold and warm seasons. Although local moisture sources play a comparable role to external sources during the cold season, external sources dominate in the warm season. Extreme moisture transport events are also becoming more intense, driven predominantly by external sources. Our findings emphasize the long-distance transport nature of Arctic ARs and provide valuable insights into their potential future changes under a warming climate.

1. Introduction

Against the backdrop of global warming, the Arctic is experiencing dramatic changes, with its surface temperature rising three to four times faster than the global average due to both external forcing and internal variability (Chylek et al., 2022; Rantanen et al., 2022; Sweeney et al., 2023), a phenomenon known as Arctic Amplification (AA). Alongside the rapid increase in surface air temperature, the Arctic sea ice extent has been shrinking at an unprecedented rate (Wang et al., 2022). Since 1979, the Arctic sea ice minimum extent in September has been declining at a rate of ~12.2% per decade (NASA, 2021), and it is expected that the Arctic will experience ice-free summers by the mid-21st-century (Årthun et al., 2021; Jahn et al., 2024). These ongoing changes have profound implications for both local human activities and the Earth system (Amstrup et al., 2010; Ford et al., 2021; Meier et al., 2014; Post et al., 2013; von Deimling et al., 2021). Given the impacts of AA, significant research efforts have been devoted to understanding the mechanisms driving this phenomenon. In particular, previous studies have underscored the role of atmospheric latent heat or water vapor transport in the winter AA observed in recent decades (Graversen & Burtu, 2016) and identified the critical contribution of downward longwave radiation to the recent Arctic surface warming trend, especially in the cold season (Zhang et al., 2021) when the increased Arctic moisture plays an important role.

Moisture transported into the Arctic predominantly occurs via the eddy component of the atmospheric circulation (Dufour et al., 2016). Recent studies have highlighted that atmospheric rivers (ARs)—long, narrow filaments of intense moisture transport—are responsible for a substantial portion of this moisture influx, contributing up to 70%–80% of the total atmospheric moisture transported into the Arctic, depending on the detection algorithm (Liu & Barnes, 2015; Woods et al., 2013; C. Zhang et al., 2023; P. Zhang et al., 2023) which suggests that ARs may contribute significantly to AA. Traditionally, ARs were considered a mid-latitude phenomenon due to their prevalence in those regions and their importance in regional hydrological cycles (Payne et al., 2020). For example, ARs provide critical freshwater to many coastal regions and can end prolonged droughts (Dettinger et al., 2011; Lavers & Villarini, 2015; Rutz & Steenburgh, 2012). However, they can also drive extreme weather events such as heavy precipitation (Lavers & Villarini, 2013; Leung & Qian, 2009; Ma, Chen, & Guan, 2020; Ma, Norris, & Chen, 2020), flooding (Corringham et al., 2019; Ralph et al., 2006), landslides (Cordeira et al., 2019; Rutllant et al., 2023), and compound extreme events (Waliser & Guan, 2017). As AR research expands into the Arctic, increasing evidence points to their substantial influence on the region's hydrological and energy budgets. Over synoptic timescales, ARs are major drivers of extreme precipitation (Serreze et al., 2015, 2022) and heat events (Ma, Wang, Chen, Qian, et al., 2024; Woods & Caballero, 2016) in the Arctic due to the large amounts of heat and moisture they deliver. The enhanced downward longwave radiation associated with ARs can accelerate the melting of sea ice and Greenland Ice Sheet (Hegyi & Taylor, 2018; Li et al., 2024; Mattingly et al., 2018; C. Zhang et al., 2023; P. Zhang et al., 2023).

The variability of ARs in the Arctic or elsewhere is governed by two main factors: (a) large-scale circulation variability, and (b) variability in atmospheric moisture (Ma & Chen, 2022; Ma, Chen, & Guan, 2020; Ma, Norris, & Chen, 2020; Ma, Wang, Chen, Leung, et al., 2024; Ma et al., 2021). Although previous studies have largely focused on the role of large-scale circulation, such as the influence of atmospheric blocking and the combined effect of the positive North Atlantic Oscillation and Ural Blocking (Luo et al., 2017; Murto et al., 2022; Papritz et al., 2022), little attention has been given to the variability in AR moisture sources. Understanding where Arctic ARs source their moisture is crucial to evaluating their formation and impact. Using a Lagrangian back trajectory approach, Vázquez et al. (2018) identified the North Pacific and North Atlantic, particularly the western boundary current regions, as major year-round moisture sources for Arctic ARs, with continental sources gaining importance during summer. However, their study focused on ARs affecting a 10° latitude band centered at 60°N, which mostly covers land and relatively warm ocean regions. These ARs do not necessarily impact further poleward sea ice regions. Additionally, Vázquez et al. (2018) did not provide a detailed examination of how AR characteristics influence their source attribution, and the analysis was limited to 1997–2014, precluding trend analysis. The Lagrangian approach also neglects some subgrid-scale physical processes and airmass (parcel) mixing, leading to increased uncertainties in long range moisture transport (Gimeno et al., 2012; Sodemann et al., 2008).

To address these limitations, this study employs an Eulerian moisture-tagging method to track the sources of moisture for ARs occurring north of 70°N. Compared to Lagrangian trajectory-based methods, the moisture-tagging approach implemented within a climate model benefits from a more comprehensive representation of atmospheric processes, allowing for a more realistic simulation of water phase change and moisture transport. This enables a more physically consistent and accurate attribution of moisture sources. This tagging method has been widely applied to identify moisture sources for precipitation over regions such as Antarctica (Wang et al., 2020), Central Asia (Jiang et al., 2020), East Asia (Pan et al., 2017), North America (Bosilovich et al., 2003), and Europe (Sodemann et al., 2009), as well as globally (H. A. Singh et al., 2016; H. K. A. Singh et al., 2016). It has also been used to study AR moisture sources affecting the west coasts of North America and Europe (Eiras-Barca et al., 2017; Hu & Dominguez, 2019; Nusbaumer & Noone, 2018; Sodemann & Stohl, 2013). By assigning unique tags to predefined source regions, the method tracks moisture from its individual evaporation regions to its eventual precipitation at the surface. Using the Community Atmosphere Model version 5 (CAM5), equipped with the moisture-tagging capability, this study seeks to address three key questions: (a) Where do Arctic ARs source their moisture, and do the major source regions vary with AR intensity? (b) How do the origins (i.e., initial detection location) and transport pathways of Arctic ARs influence the spatial distribution of their moisture sources? (c) Which source regions contribute to the observed moistening trends of the mean state and extreme transport events over the Arctic since 1980?

The remainder of this paper is organized as follows: Section 2 describes the AR detection algorithm, trajectory clustering method, and the design of the CAM5 moisture-tagging simulation. Section 3 presents the main results, including the identification of source regions for Arctic ARs in the Atlantic and Pacific sectors and comparison with climatological moisture and precipitation sources. We also explore the dependency of moisture sources on the vertical atmospheric levels and intensity of AR, as well as their origins and pathways using trajectory clustering analysis. Finally, we identify and quantify the source regions contributing to the recent Arctic wetting. Section 4 summarizes the major findings, discusses their implications, and suggests directions for future research.

2. Data and Methods

2.1. AR Detection Algorithm

Historically, most AR studies have focused on the midlatitudes, and as a result, most global AR detection algorithms have been optimized for identifying ARs in those regions. These algorithms often detect very few ARs in the polar regions due to their design, which can limit their effectiveness in high latitudes. Algorithms specifically tuned for Arctic conditions remain limited, with notable examples including Mattingly et al. (2018) and Wille et al. (2021). In this study, we also perform an AR trajectory clustering analysis, which requires consistent AR detection at both high latitudes and the lower-latitude source regions where ARs typically originate. Given these constraints, we select an algorithm that is capable of tracking ARs globally and continuously over their lifespan. To detect Arctic ARs, we employ the integrated water vapor transport (IVT)-based global AR detection algorithm developed by Guan and Waliser (2019) with a minor modification. This algorithm is an updated version of the widely used AR detection method originally proposed by Guan and Waliser (2015). The identification process involves several key steps. First, a seasonally and regionally dependent 85th percentile IVT magnitude, combined with a lower-bound of 100 kg m^{-1} s^{-1}, is used to extract contiguous regions exceeding this threshold. Additional criteria, such as IVT direction coherence, mean poleward IVT magnitude, length requirements, and the length-to-width ratio, are subsequently applied. Only objects meeting these criteria are identified as ARs. This combination of relative and absolute thresholds allows for a reasonable detection of ARs in the Arctic and is recommended by the Atmospheric River Tracking Method Intercomparison Project (ARTMIP) for high-latitude AR research (Rutz et al., 2019). A key update in the Guan and Waliser (2019) algorithm enables the spatio-temporal tracking of individual ARs by linking the centroid location of ARs at each time step, thereby identifying AR trajectories. These trajectories are used as input to a clustering algorithm to investigate how the source regions of Arctic ARs depend on their origins and travel paths. Since ARs reaching the Arctic are typically near the end of their lifecycle, we follow Mattingly et al. (2018) and relax the length requirement from 2,000 to 1,500 km. Further details are referred to Guan and Waliser (2019).

We use 6-hourly IVT data at 00, 06, 12, and 18 UTC as input for the algorithm. The zonal and meridional IVT components were computed by vertically integrating the moisture flux at 1000, 850, 700, and 500 mb using the following equations:

$$\text{Zonal IVT} = \frac{1}{g}\int_{1000}^{500} uq\, dp$$

$$\text{Meridional IVT} = \frac{1}{g}\int_{1000}^{500} vq\, dp$$

where g is gravitational acceleration, u and v are the zonal and meridional wind components, respectively, and q is specific humidity.

2.2. AR Trajectory Clustering Algorithm

To classify AR trajectories, we apply the trajectory clustering algorithm developed by Gaffney et al. (2007). This method, based on a finite mixture model, represents the data distribution as a convex linear combination of component density functions. The algorithm clusters trajectories according to their genesis location and the

10.1029/2025JD043918

geometric shape of their paths. Following Li et al. (2023), we use a quadratic polynomial density function to model the AR trajectories, assuming that each trajectory was generated by one of K regression models (where K is the number of clusters). Each trajectory is assigned to the regression model with the highest probability of generating it. This method has been widely used for studying tropical cyclone tracks (Camargo et al., 2007a, 2007b; Mei & Xie, 2016) and has also been applied to AR trajectories over the North Atlantic (Li et al., 2023). To ensure regional specificity, we divide AR trajectories into those reaching the Atlantic sector of the Arctic (70°N–80°N, 20°W–40°E) and those reaching the Pacific sector of the Arctic (70°N–80°N, 150°E−150°W). For each sector and season, we test cluster sizes ranging from four to eight and select the smallest number of clusters that adequately captures the diversity of AR trajectories while maintaining clarity and interpretability. This results in six clusters for the cold season and seven for the warm season. These clusters represent key variations in AR genesis locations and pathways. Further details on the clustering algorithm are referred to Gaffney et al. (2007).

2.3. Model Description and Experiment Setup

This study uses the CAM5 model, which is the atmospheric component of the Community Earth System Model version 1 (CESM1) (Hurrell et al., 2013), equipped with an atmospheric moisture-tagging capability to identify moisture source regions for Arctic ARs (Nusbaumer et al., 2017). CAM5 has been widely used in source attribution studies for precipitation and AR moisture over various regions (Jiang et al., 2020; Nusbaumer & Noone, 2018; Pan et al., 2017; H. A. Singh et al., 2016; H. K. A. Singh et al., 2016; Wang et al., 2020) and provides a reasonable representation of atmospheric hydrological processes involving evaporation, clouds, precipitation, and large-scale circulation (Neale et al., 2010). CAM5 is run with a horizontal resolution of 1.9° latitude by 2.5° longitude and 30 vertical levels. The "atmosphere-only" setup, with prescribed historical monthly sea surface temperatures (SSTs) and sea ice concentrations coupled with the interactive land model (CLM4) (Oleson, 2010), is used to simulate the period from 1979 to 2021. The year 1979 is excluded from the analysis as a model spin-up. Boundary forcing data for SST and sea ice are based on NOAA's Extended Reconstructed SST version 5 (ERSSTv5; Huang et al., 2017). The simulation is conducted with historical forcing from 1979 to 2014 and Representative Concentration Pathways 4.5 (RCP4.5) forcing thereafter.

The variability of large-scale circulation exerts strong controls on the formation of Arctic ARs and atmospheric moisture transported into the Arctic (Ma, Wang, Chen, Leung, et al., 2024; Murto et al., 2022; Papritz et al., 2022). Climate models, including CESM1, still have deficiencies in representing large-scale circulation, undermining the robustness of source attribution results (Simpson et al., 2020). To correct such biases in large-scale circulation, following Zhang et al. (2022), the large-scale circulation (zonal and meridional winds above ~900 mb) is nudged toward the European Centre for Medium-Range Weather Forecasts Reanalysis, version 5 (ERA5; Hersbach et al., 2020) reanalysis data with a 6-hr relaxation timescale. This ensures that the model's large-scale circulation variability matches the observational data. Combined with the observed boundary forcing, the model setup used in this study is especially suitable for decadal trend analysis.

To apply the moisture-tagging capability to Arctic ARs source attribution, we define 33 source regions (Figure 1) and assign tags to the moisture originating from each. The Arctic, mid-, and high-latitude regions of the Northern Hemisphere are divided into smaller tagged regions to enable detailed quantification of their contributions. The Southern Hemisphere, having a minor contribution, is divided into just two tags: land and ocean. For each regional tag, a set of new water variables (e.g., mass mixing ratio of vapor, cloud liquid, cloud ice, stratiform and convective precipitation) are defined and tracked from their evaporation or sublimation sources to their sink regions, where they return to the Earth's surface in the form of condensate or precipitation. These tracers are treated in the same way as the standard global water variables, undergoing the same atmospheric parameterizations and processes (e.g., convection, cloud microphysics, advection, and boundary layer mixing). More details on water tracers in CAM5 can be found in Nusbaumer et al. (2017).

3. Results

3.1. Moisture Sources for the Arctic Hydrological Cycle

The accuracy of source attribution depends heavily on the model's ability to simulate both the variability and mean state of large-scale circulation and moisture. Since the model wind field is nudged toward observations, biases in large-scale circulation are negligible (not shown). As shown in Figure S1 in Supporting Information S1, CAM5 exhibits a general wet bias globally, with larger integrated water vapor (IWV) biases over the lower-

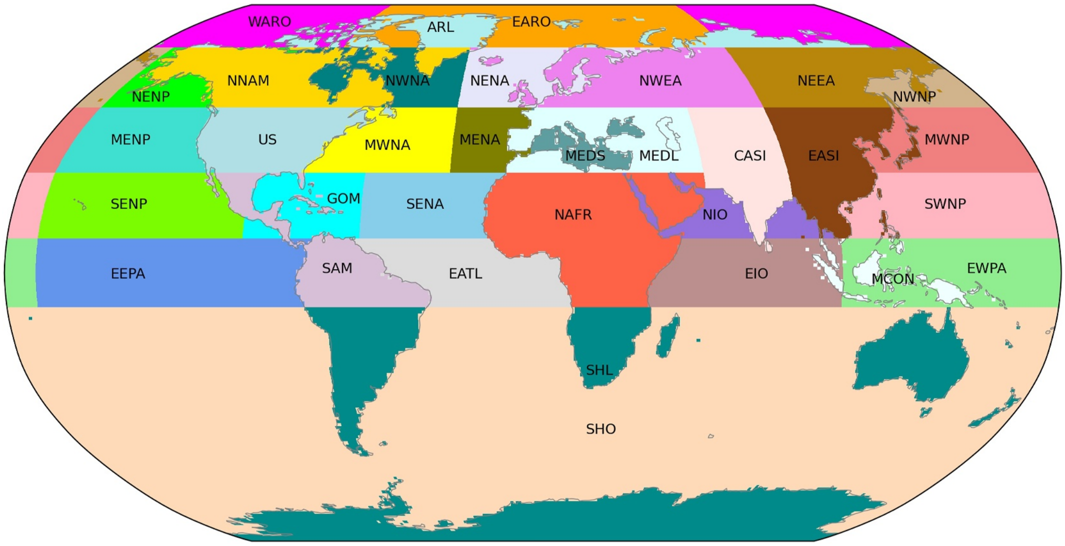

Figure 1. Thirty-three moisture source regions that are tagged in this study (see Table S1 in Supporting Information S1 for their definitions).

latitude subtropical and tropical regions (Figure S1d in Supporting Information S1), consistent with the previous evaluation of CAM5 (Nusbaumer et al., 2017). In the Northern Hemisphere, IWV biases vary seasonally. During the cold season (November–March; Figure S1e in Supporting Information S1), strong moist biases are mainly confined to the tropics, although biases in the Arctic are relatively small. In the warm season (May–September; Figure S1f in Supporting Information S1), positive IWV biases shift poleward, with the largest biases observed over mid- and high latitudes. The Arctic also suffers a wet bias. As shown later, the Northern Hemisphere high-latitude continents serve as important moisture sources for the Arctic. Such a warm-season wet bias over the Arctic could be caused by biases in simulating evaporation by the CESM1 land model. Consistent with the Arctic's wet bias, CAM5 also tends to overestimate Arctic AR frequency (Figure S2 in Supporting Information S1). During the cold season (Figure S2e in Supporting Information S1), positive biases occur in the peak climatological AR frequency regions of the Pacific and Atlantic sectors. In this season, the 85th percentile IVT threshold is often lower than 100 kg m^{-1} s^{-1}; thus, 100 kg m^{-1} s^{-1} effectively becomes the threshold, leading to a positive bias in AR frequency. In the warm season, the 85th percentile IVT exceeds 100 kg m^{-1} s^{-1} across most of the Arctic, except Greenland. Consequently, positive AR frequency biases are mostly confined to Greenland, although biases in other Arctic regions are minimal. Given these IWV and AR frequency biases, any quantification of source contributions in absolute terms is likely overestimated. Thus, this study focuses on the fractional contributions from different source regions.

3.1.1. Source Attribution for Arctic Climatological Moisture and Precipitation

To contextualize Arctic AR moisture sources, we first quantify the fractional contributions of source regions to the climatological Arctic moisture (Figure 2) and precipitation (Figure 3). Analyses are conducted for the cold season (November–March) and warm season (May–September), respectively. Since ARs primarily enter the Arctic via the Atlantic and Pacific pathways (Figures S2 and S3 in Supporting Information S1), detailed analyses are focused on the Atlantic sector (70°N–80°N, 20°W–40°E) and the Pacific sector (70°N–80°N, 150°–E−150°W). During the cold season, the Arctic predominantly sources moisture from the North Atlantic (poleward of 10°N), the North Pacific (poleward of 10°N), and the local Arctic, particularly the Eastern Arctic Ocean (Figure 2a). These regions contribute approximately 37.2%, 28.3%, and 17.7%, respectively, to the Arctic climatological, vertically integrated moisture. Other Northern Hemisphere continental regions, except northwest Eurasia and the Mediterranean basin, contribute minimally. In the warm season, the locally sourced moisture becomes less significant, with its fractional contribution dropping from 17.7% to 11.7% (Figures 2d and 2g). This decrease is mainly due to reduced moisture from the Eastern Arctic Ocean, although contributions from the Western Arctic Ocean and Arctic land increase. Land-based sources, particularly from the high-latitude North America and Eurasia, increase substantially, with mid- and high-latitude Northern Hemisphere continents

10.1029/2025JD043918

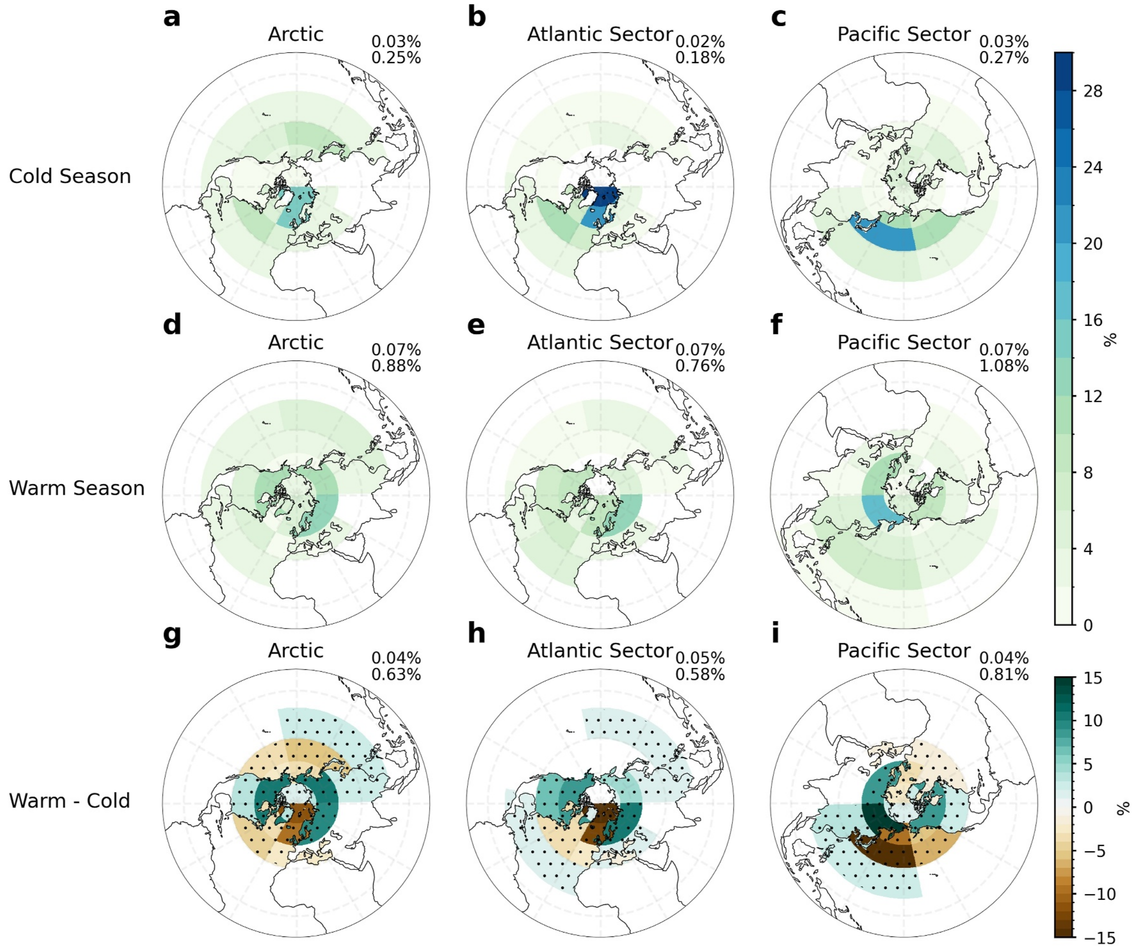

Figure 2. Fractional contribution from each source region to the spatially averaged cold-season integrated water vapor (IWV) is shown in the top-row panels (a–c). Middle-row panels (d–f) display the same information but for the warm season. The corresponding differences between the warm and cold seasons (warm–cold) are shown in panels (g–i). The left, middle, and right columns present the results for the entire Arctic (poleward of 70°N), Atlantic sector (70°N–80°N, 20°W–40°E), and Pacific sector (70°N–80°N, 150°E−150°W), respectively. Stippled areas in (g–i) indicate significant differences at the 0.05 level based on the Student's *t*-test. Regions where the magnitude of the values is less than 1% have been masked out. The values in the upper right of each panel indicate the fractional contributions from Southern Hemisphere land (top value) and ocean (bottom value) for panels (a–f), and their seasonal differences for panels (g–i). Bolded values in panels (g–i) indicate statistically significant differences at the 0.05 level.

contributing 47.9% to the Arctic moisture. Meanwhile, contributions from the North Atlantic and North Pacific decreased to 17.8% and 16.5%, respectively.

Focusing on the Atlantic sector, locally sourced moisture from the Eastern Arctic Ocean makes up 29.3% of the climatological moisture in the cold season (Figure 2b), likely due to the partially open ocean underneath, which creates a stronger vertical gradient in temperature and humidity near the sea surface. The rest of the moisture is predominantly drawn from the North Atlantic, with a fractional contribution of 49.7%. Interestingly, the region between 10°N and 50°N over the North Pacific contributes about 7.2% to the mean moisture over the Atlantic sector. Further analyses suggest that this Pacific-sourced moisture is first transported into the North Atlantic through the westerlies and then advected meridionally into the Atlantic sector (not shown). Similar to the climatological moisture over the entire Arctic, locally sourced moisture and contributions from the North Atlantic become less significant during the warm season, however the contribution from land increases noticeably (Figures 2e and 2h). In this season, the Arctic, North Atlantic, and Northern mid- and high-latitude continents are the three primary sources for the Atlantic sector, contributing about 12.2%, 31.5%, and 40.6% to the climatological moisture.

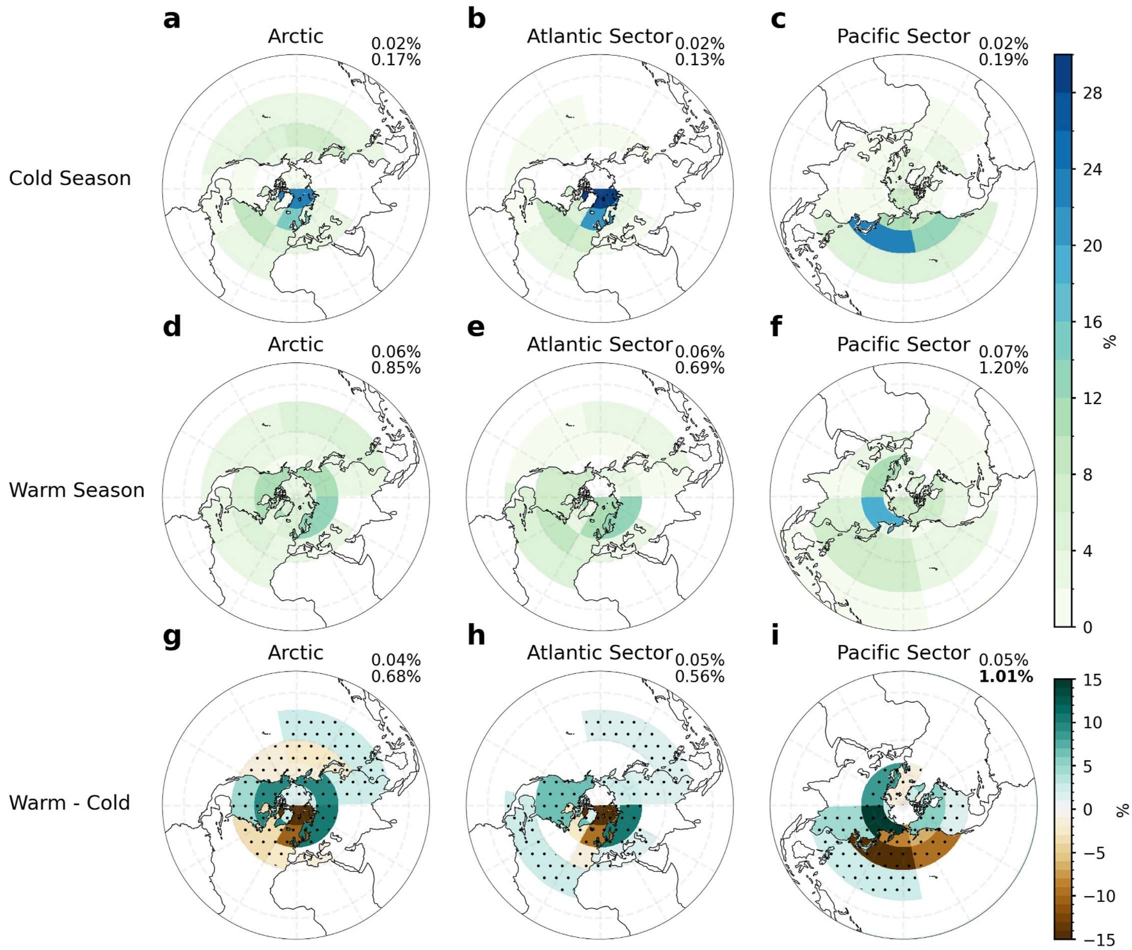

Figure 3. Same as Figure 2, but for the fractional contribution to mean precipitation at the surface.

In the Pacific sector, local moisture from the Western Arctic Ocean contributes only 2.6% during the cold season (Figure 2c), likely due to a complete sea ice cover. Moisture is primarily sourced from the North Pacific (59.2%), followed by 17.4% originating from the North Atlantic. Further analyses show that the North Atlantic-sourced moisture enters the Pacific sector through a cross-Arctic pathway (not shown). In the warm season, local contribution from the Western Arctic Ocean increases to 4.3%, likely due to sea ice melt. Similar to contributions to the Arctic and Atlantic sectors, the North Pacific contribution declines in the warm season, however land-based sources rise, with contributions of 24.9% and 49.5%, respectively. Remote sources, such as the subtropical oceans, also strengthen during the warm season for all regions (Figures 2g–2i). Notably, the Pacific sector even receives discernable contributions from the Southern Hemisphere (Figure 2f), likely due to longer atmospheric moisture residence times in the warm season.

Previous studies indicate that moisture entry altitude into the Arctic depends on source regions (Papritz et al., 2022; Wang et al., 2020). Indeed, our results (Figures S4 and S5 in Supporting Information S1) show a strong altitude dependency. At lower altitudes (1,000–850 mb), moisture is primarily sourced locally and from nearby oceans (and nearby continents in the warm season). As altitude increases, remote sources dominate, and local contributions in the Arctic become negligible at 500 mb and above. At 100 mb, moisture sources are dominated by the subtropics, tropics, and the Southern Hemisphere, with no seasonal or regional dependency, indicating long residence times and well-mixed moisture there.

For precipitation, fractional contributions show similar spatial patterns to moisture (Figure 3), although precipitation draws a larger fraction of moisture locally and from adjacent regions. For instance, during the cold season, local contributions to moisture are 17.7%, 29.3%, and 2.6% for the Arctic, Atlantic sector, and Pacific sector,

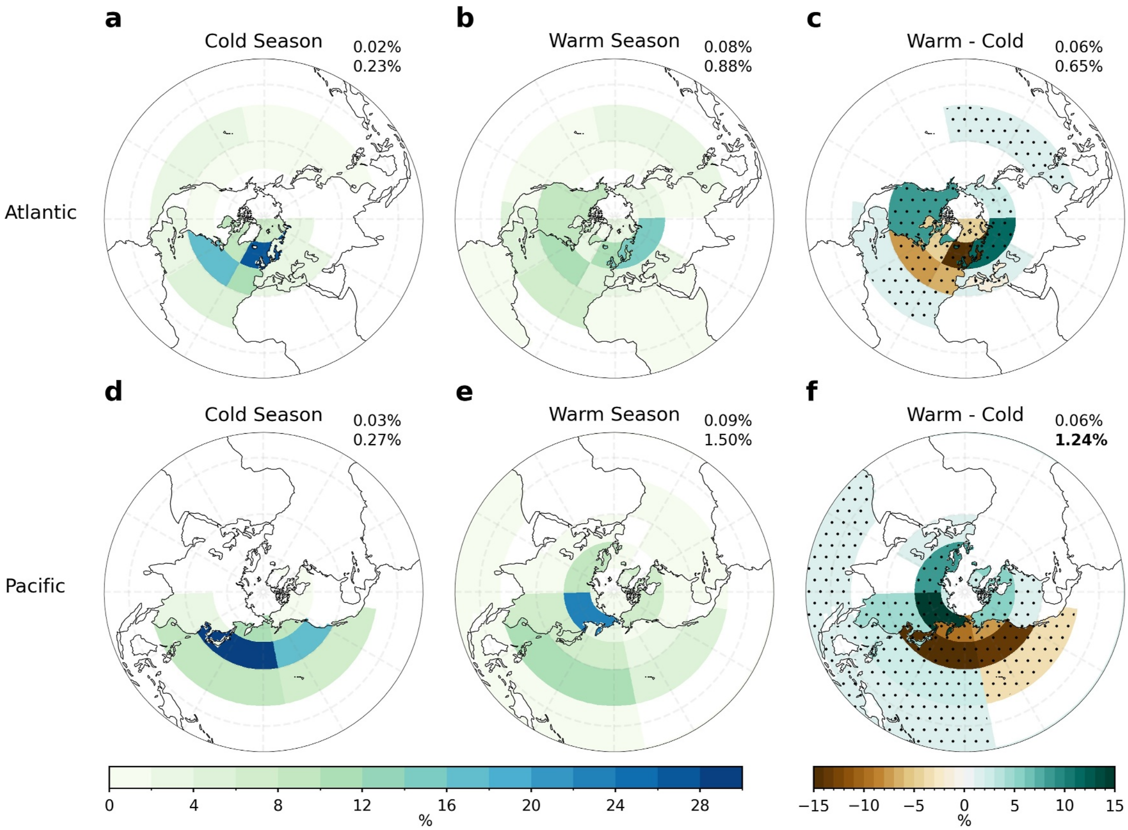

Figure 4. Fractional contribution from each source region to the cold-season AR-associated integrated water vapor (IWV) averaged over the Atlantic sector (a) and Pacific sector (d) in the Arctic. Panels (b, e) show the same information as (a, d), but for the warm season. The differences between the warm and cold seasons (warm–cold) are shown in (c, f) for the Atlantic and Pacific sectors, respectively. Stippled areas in (c, f) indicate significant differences at the 0.05 level based on the Student's *t*-test. Regions where the magnitude of the values is less than 1% have been masked out. The values in the upper right of each panel indicate the fractional contributions from Southern Hemisphere land (top value) and ocean (bottom value) for panels (a–b) and (d–e), and their seasonal differences for panels (c) and (f). Bolded values in panels (c, f) indicate statistically significant differences at the 0.05 level. Note that the central longitudes in panels (a–c) differ from those in panels (d–f).

respectively, but increase to 26.8%, 37.1%, and 7.0% for precipitation. This increase is likely due to the prevalence of precipitation-producing low clouds in these regions (Curry et al., 1996), which primarily draw moisture from nearby sources. Based on the 6-hourly precipitation data, the dependency of fractional contribution on the spatially averaged precipitation intensity over the Atlantic and Pacific sectors is also investigated (Figure S6 in Supporting Information S1). Regardless of the seasons and sectors examined, as precipitation intensity increases, local contributions decrease, while more remote oceanic sources become increasingly important. However, the contribution of land-based sources shows little sensitivity to precipitation intensity. Further analyses indicate that these extreme precipitation events in both sectors are associated with a surface low-pressure system and a filament of enhanced IVT intruding into the Arctic from lower-latitude oceanic regions (not shown). Furthermore, the increasing precipitation intensity is coincident with the deepening of low-pressure systems and the strengthening of IVT. These results suggest that extreme precipitation over the Atlantic and Pacific sectors is likely driven by ARs that source their moisture primarily from the oceans.

3.1.2. Source Attribution for Arctic AR Moisture

As shown in Figures S2 and S3 in Supporting Information S1, ARs primarily enter the Arctic through the Atlantic and Pacific pathways, with the Baffin Bay pathway also becoming prominent during the warm season. Based on the AR detection algorithm used in this study, ARs contribute over 40% of the poleward moisture flux at 70°N in the Atlantic and Pacific sectors, and in Baffin Bay during the warm season (Figure S3 in Supporting Information S1). Outside these three pathways, the AR contribution generally exceeds 30% in the warm season but falls below 20% in the cold season. Given the substantial year-round AR contribution in the Atlantic and Pacific pathways, these two sectors are the focus for the source attribution of Arctic ARs (Figure 4). AR moisture is

10.1029/2025JD043918

defined as the moisture within the AR boundaries in the respective sector. Similar to the source attribution for Arctic climatological moisture and precipitation, during the warm season Arctic ARs tend to source moisture from more remote oceanic regions and Northern Hemisphere continents, while local and nearby oceanic contributions become less significant (Figures 4c and 4f). However, for ARs, the contribution from Arctic local sources decreases substantially, while the contribution from oceanic sources within the respective extra-polar ocean basins increases and becomes dominant. For the Atlantic (Pacific) sector, the local contribution from the Eastern (Western) Arctic Ocean is 7.4% (0.9%) and 2.9% (1.9%) for the cold and warm seasons, respectively, compared to 29.3% (2.6%) and 8.9% (4.3%) for climatological moisture. Meanwhile, the contribution from oceanic sources within the respective ocean basins becomes more significant. The North Atlantic (Pacific) poleward of 10°N contributes 73.2% (85.3%) and 41.3% (29.4%) to Arctic AR moisture in the Atlantic (Pacific) sector during the cold and warm seasons, respectively. In contrast, for the Arctic climatological moisture, the contributions drop to 49.7% (59.2%) and 31.5% (24.9%) during the cold and warm seasons, respectively, over the Atlantic (Pacific) sector. Similar to climatological moisture and precipitation, land-based moisture sources become important during the warm season. For instance, mid- and high-latitude continents contribute significantly, accounting for 40.1% and 51.3% of AR moisture in the Atlantic and Pacific sectors, respectively. Additionally, as shown later, the spatial distribution of fractional contributions reflects, to some extent, the genesis locations and propagation pathways of ARs before entering the respective Arctic sectors. For example, enhanced contributions are seen over the mid-latitude western and northeastern North Atlantic for Atlantic sector ARs in both seasons (Figures 4a and 4b), suggesting that most ARs follow a southwest-to-northeast pathway. Similarly, as discussed in the next section, the more complex spatial distribution of fractional contributions for the Pacific sector AR moisture results from differences in AR genesis locations and propagation pathways affecting this sector.

To investigate whether the spatial distribution of fractional contributions depends on AR intensity, we first calculate the average poleward moisture flux across 70°N for each 6-hourly time step, separately for the Atlantic (20°W–40°E) and Pacific (150°E−150°W) sectors, and then derive their magnitudes at various percentiles. We subsequently define ARs with intensities at the 90th, 95th, and 99th percentiles as those with an averaged poleward moisture flux at 70°N between the 90th and 91st percentiles, 95th and 96th percentiles, and above the 99th percentile, respectively. AR moisture is then defined as the moisture within the Atlantic and Pacific sectors when the above criteria are met.

As shown in Figures 5 and 6, as ARs strengthen, local contributions decline while contributions from more remote oceanic sources increase. This variation in fractional contributions with AR intensity is very similar to that observed for precipitation, further suggesting that ARs play a crucial role in driving Arctic extreme precipitation. However, this dependency varies by both sector and season. For the warm season, the Pacific sector shows greater sensitivity compared to the Atlantic sector. The cold season generally exhibits higher sensitivity compared to the warm season. For example, the more remote North Atlantic between 10°N and 50°N contributes 27.4%, 30.7%, and 38.5% to the cold-season Atlantic sector moisture for ARs with intensities at the 90th, 95th, and 99th percentiles, respectively. However, in the warm season, these contributions decrease to 23.2%, 24.8%, and 26.4%, respectively. This reduced sensitivity for the Atlantic sector in the warm season is likely due to both an increase in moisture residence time at higher temperatures and the relatively smaller spatial extent of the Atlantic basin compared to the Pacific, resulting in a better mixing of moisture.

Similar to that for the Arctic climatological moisture, the spatial distribution of fractional contributions associated with Arctic ARs also shows altitude dependency (Figure S7 in Supporting Information S1). As altitude increases from 1,000 mb to 250 mb, Arctic local contributions decrease, while ARs source moisture from increasingly remote oceanic regions during the cold season and from both oceanic and continental regions during the warm season. Compared to moisture sources for the climatological moisture, Arctic ARs uptake less moisture locally and more from remote sources at every pressure level below 250 mb. At 100 mb, the source distribution is again independent of both season and sector, closely resembling that of the climatological moisture (compare Figure S7 in Supporting Information S1 with Figures S4 and S5 in Supporting Information S1), suggesting that the influences of ARs are largely confined to the troposphere.

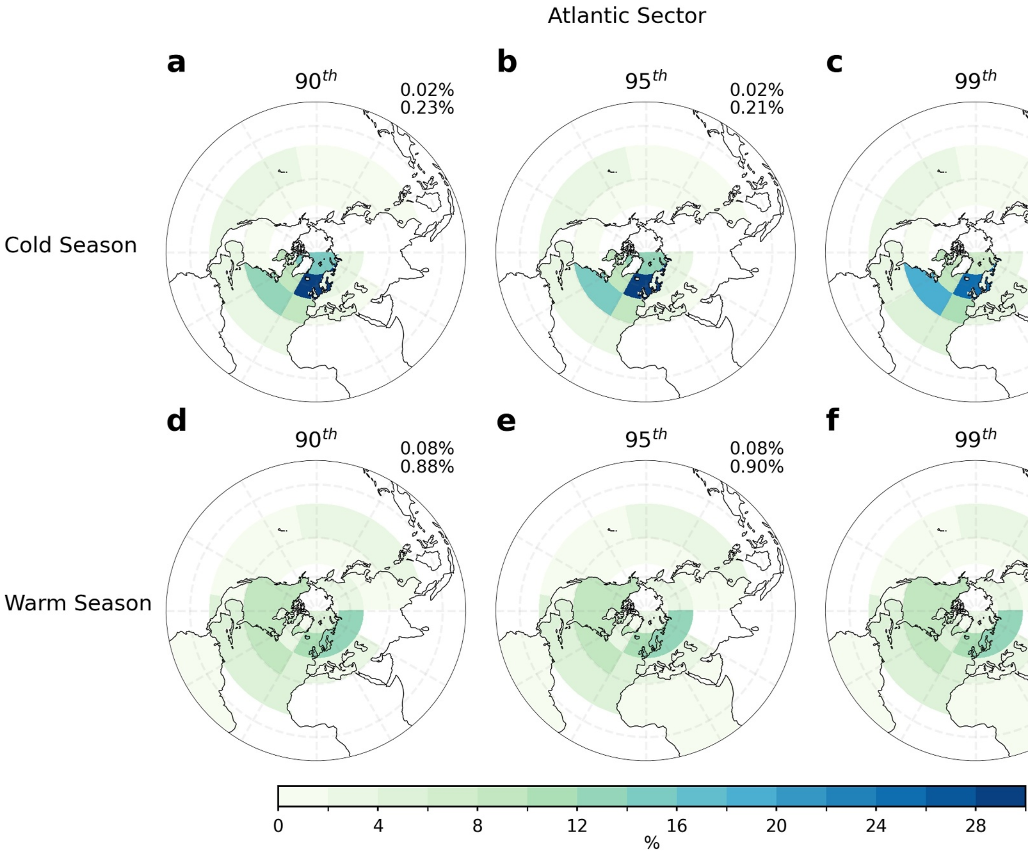

Figure 5. Dependency of the fractional contribution from each source region to the Atlantic sector integrated water vapor (IWV) on AR intensity for the cold season (a–c) and warm season (d–f). The left, middle, and right columns are for ARs with intensities at the 90th, 95th, and 99th percentiles, respectively (see text for the definition of AR intensity). Regions where the magnitude of the values is less than 1% have been masked out. The values in the upper right of each panel indicate the fractional contributions from Southern Hemisphere land (top value) and ocean (bottom value).

3.2. AR Clustering Analyses

Arctic ARs vary in their genesis locations and propagation pathways before entering the Arctic. Previous source attribution studies for mid-latitude landfalling ARs have shown that ARs with tropical or subtropical origins typically lose most of their moisture sourced from the origin via precipitation along their transport pathways, with only a small fraction reaching their landfall destinations (Bao et al., 2006; Dacre et al., 2015; Hu & Dominguez, 2019; Sodemann & Stohl, 2013). Moisture convergence and evaporation along their pathways are important mechanisms for replenishing AR moisture content. Compared to mid-latitude ARs, Arctic ARs encounter very different environmental conditions, characterized by a colder and drier atmosphere along their pathways. Additionally, depending on the season and sector, their final destination can be fully or partially sea-ice-covered regions or open ocean. To determine whether the moisture uptake mechanisms observed in mid-latitude ARs also apply to Arctic ARs, we use a trajectory clustering technique to divide Arctic AR trajectories into distinct clusters and investigate how the spatial distribution of fractional contributions depends on AR genesis locations and propagation pathways (Figures 7 and 8).

In the cold season, ARs reaching the Atlantic sector can be broadly divided into six clusters, each characterized by distinct AR genesis locations and propagation pathways (Figures 7a–7f). For example, clusters 1–3 originate from mid- and high-latitude regions, while clusters 4–6 have subtropical origins (Figure S8 in Supporting Information S1). Consistent with that of mid-latitude ARs, the moisture source for Arctic ARs also exhibits a dependency on their genesis location and pathway. For instance, ARs in cluster two originate from and/or propagate along mid-latitude western Europe (Figure S8b in Supporting Information S1). Consequently, increased moisture is sourced from the mid-latitude eastern North Atlantic, western Europe, and the Eastern Arctic Ocean, while the contribution from the western North Atlantic decreases (Figure 7b). Interestingly, clusters 4 and 6, which have

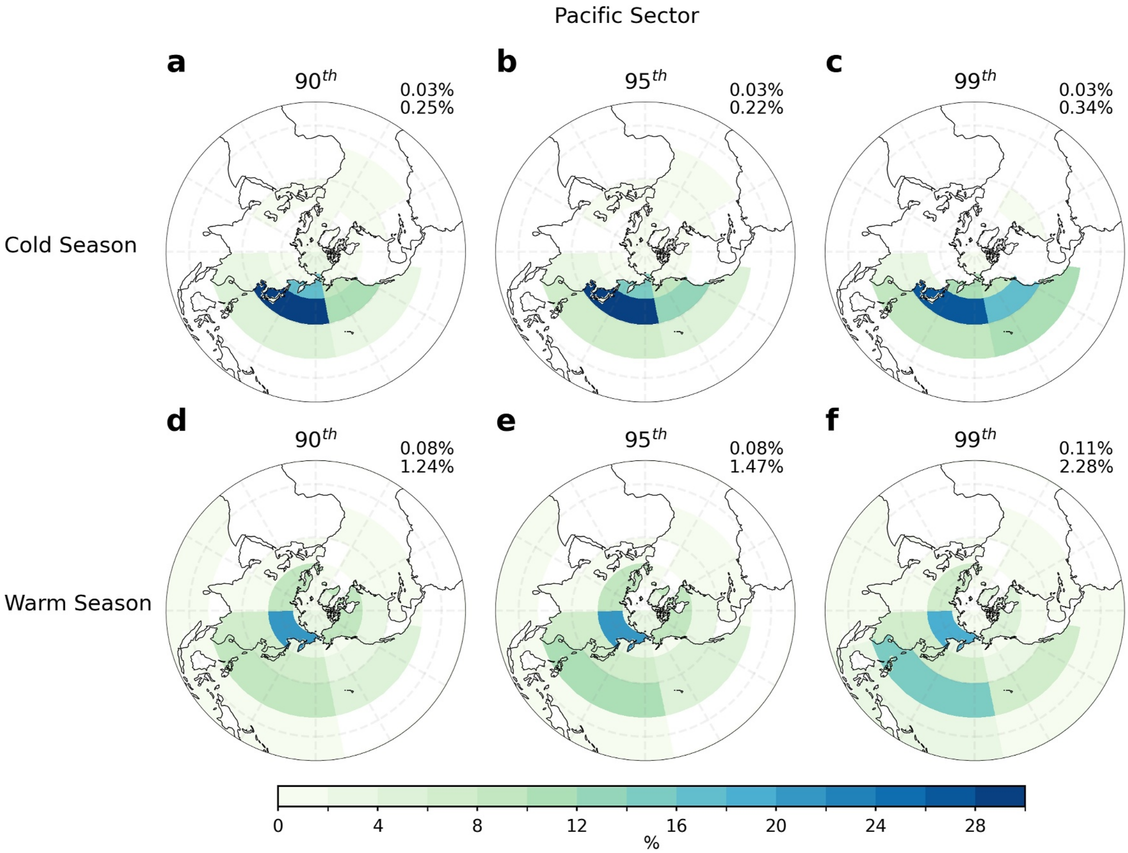

Figure 6. Same as Figure 5, but for the Pacific sector.

subtropical origins (Figures 7d and 7f), show enhanced moisture uptake over the western North Atlantic and Gulf of Mexico, indicating that long-distance transport is possible even for Arctic ARs in the cold season. Additionally, ARs with more distant oceanic origins tend to contribute disproportionately to AR-associated moisture over the Atlantic sector. For example, while clusters 4 and 6 account for only 7.7% and 14.6% of the total trajectories, they contribute 10% and 19.1% of the AR-associated moisture over the Atlantic sector, respectively. In contrast, clusters 1 and 2, which originate from regions closer to the Atlantic sector and make up 49.6% and 8.2% of the trajectories, contribute only 37% and 5.3% to the total AR moisture, respectively (Figures 7a and 7b). This outsized contribution from ARs with remote oceanic origins is likely due to a combination of warmer temperatures within the ARs, which enables them to carry more moisture, and their more meridionally oriented trajectories, allowing them to impact a larger area in the region of interest.

In the warm season, ARs can be categorized into seven clusters (Figures 7g–7m), with the trajectories in cluster 3 showing an incoherent pattern; thus, this cluster is denoted as "other." Compared to the cold season, warm-season Arctic ARs affecting the Atlantic sector generally originate from higher latitude regions (Figure S9 in Supporting Information S1). For example, clusters 1, 2, and 4, which originate from the northern high latitudes, together account for 70.1% of the total trajectories. The remaining clusters (clusters 5, 6, and 7) have mid-latitude origins. This higher-latitude origin of warm-season Arctic ARs is likely due to the poleward shift of the westerly jet, which shifts ARs toward higher latitudes. Similar to cold-season Arctic ARs, the moisture source also shows a dependency on AR origin and pathway. For instance, the trajectories in clusters 5–7 exhibit a southwest-to-northeast orientation. Correspondingly, these ARs source more moisture from North America and the North Atlantic and less from western Europe. Unlike those in the cold season, none of the clusters identified in the warm season originate from subtropical regions. However, enhanced subtropical moisture uptake is still observed in clusters 3, 4, 6, and 7, likely due to an increased residence time of moisture, which allows the moisture advection into higher latitudes and subsequently transported into the Atlantic sector in ARs. Consistent with the enhanced continental sources in the warm season, a greater fraction of Arctic ARs also originates over land. For example, a large

10.1029/2025JD043918

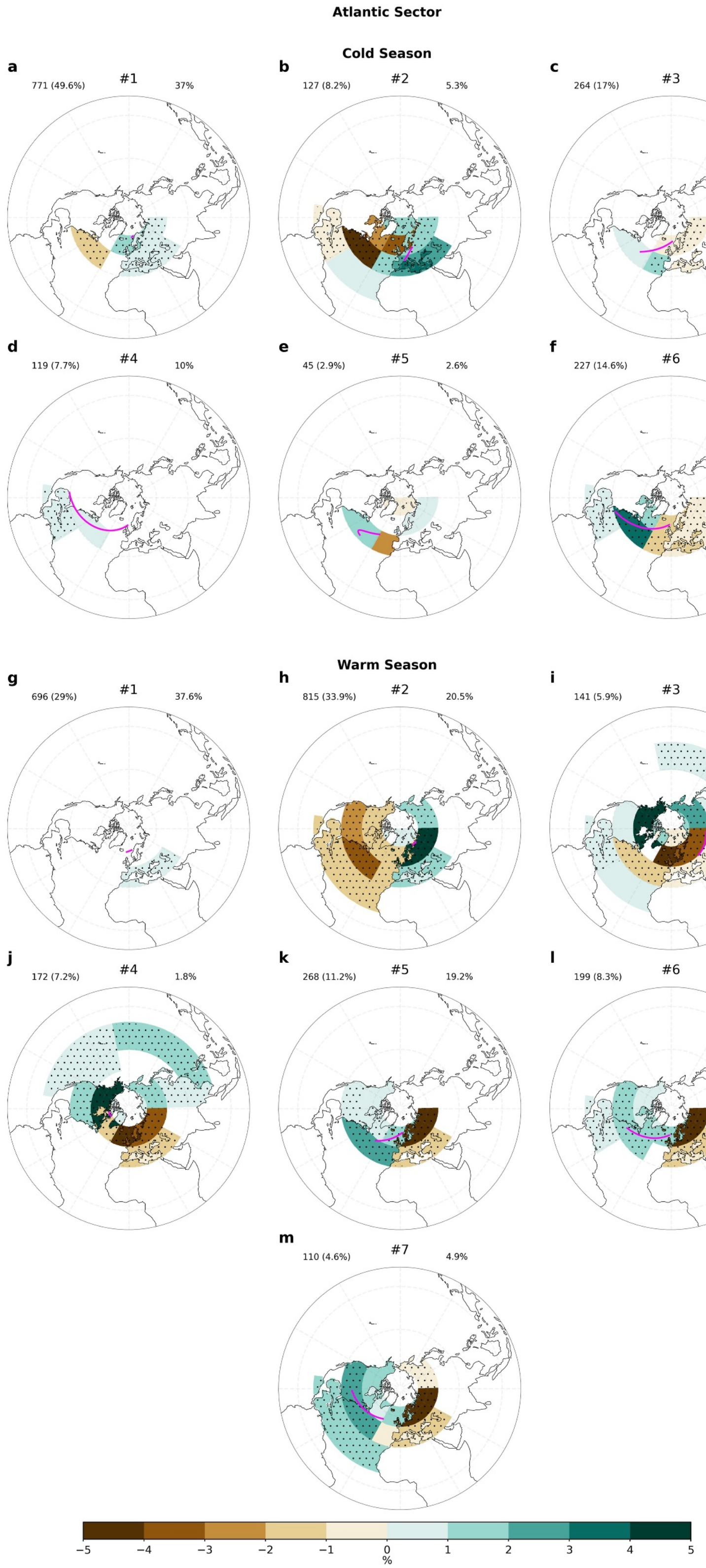

Figure 7.

portion of ARs in clusters 2, 3, 4, and 7 first appears over land, resulting in an increased moisture uptake from the continents of their origin. Previous studies have emphasized the role of enhanced continental evaporation in driving the increased contribution of continental moisture to the warm-season Arctic moisture (Gimeno et al., 2019; Singh et al., 2017; Vázquez et al., 2016, 2018). In this study, we show for the first time that the increase in Arctic ARs with a continental origin also acts as an important mechanism driving more land-based moisture into the Arctic during the warm season.

Consistent with the suppressed AR activity over the Pacific sector during the cold season (Figure S2b in Supporting Information S1), relatively few AR trajectories are identified in this season (Figures 8a–8f). Six clusters are identified for ARs affecting the Pacific sector in the cold season. Cluster 5, with only 46 trajectories, shows an incoherent pattern. The reduced contribution from the North Pacific basin and the enhanced contribution from the North Atlantic basin indicate that this cluster is associated with cross-Arctic transport by ARs from the North Atlantic into the Pacific sector (Figure S10e in Supporting Information S1). Three of the clusters (1, 3, and 6) exhibit a dipole pattern in moisture uptake anomalies over the North Pacific, characterized by enhanced uptake from one side of the basin and reduced uptake from the other. This dipole pattern is likely caused by the more meridionally oriented AR trajectories in these clusters, which result in moisture being predominantly sourced from only one side of the basin. Cluster 4 accounts for nearly half of the trajectories and contributes almost half of the AR moisture over the Pacific sector. The anomaly moisture uptake pattern associated with this cluster is nonsignificant, suggesting that the anomalous contributions of the other five clusters tend to cancel each other out, making the contribution from cluster 4 dominant.

In the warm season, seven clusters are identified (Figures 8g–8m). Similar to cluster 5 in the cold season, cluster 3 exhibits an incoherent pattern. The enhanced contribution from the North Atlantic and the reduced contribution from the North Pacific suggest that many ARs in this cluster transport moisture via a cross-Arctic route, carrying moisture from the North Atlantic into the Pacific sector. In addition to cluster 3, as shown in Figure 8h, ARs in cluster 2 also source moisture from the Atlantic sector and western Europe, resulting in an enhanced uptake over those regions and reduced uptake over the Pacific basin. Compared to the cold-season trajectories, warm-season trajectories not only occur at overall higher latitudes but also exhibit a more zonal orientation. Consequently, the dipole moisture uptake pattern observed in the cold season disappears in the warm season. For example, clusters 1, 5, and 6 are associated with basin-wide enhanced uptake, while clusters 2, 3, 4, and 7 are associated with basin-wide reduced uptake. Consistent with the increase in land-based sources, a larger fraction of ARs with continental origins is observed in the warm season, particularly in clusters 2 and 4.

3.3. Source Attribution for Arctic Moistening Trends

3.3.1. Source Attribution for Mean Arctic Moistening Trends

The rapid Arctic warming in recent decades has been accompanied by a strong moistening trend in both seasons (Figure S12 in Supporting Information S1). This trend exhibits a dipole pattern, with faster moistening over the Atlantic sector compared to the Pacific sector, particularly during the cold season. The nudged CAM5 simulation successfully reproduces both the spatial pattern and magnitude of the cold-season moistening trend (comparing Figures S12a and S12c in Supporting Information S1). However, for the warm season, while the model captures the spatial pattern well, it significantly overestimates the moistening magnitude. Given that the mid- and high-latitude continents of the Northern Hemisphere contribute nearly half of the Arctic's climatological moisture in the warm season, this overestimation may stem from deficiencies in the model's simulation of continental evaporation trends. Further analysis of the causes of this bias is beyond the scope of this study.

We first examine the fractional contribution of each source region to the mean moisture trends over the entire Arctic, the Atlantic sector, and the Pacific sector for both seasons (Figure 9). As shown in Figure 9a, the cold-

Figure 7. Differences in the fractional contribution from each source region to the AR-associated integrated water vapor (IWV) between each of the individual AR clusters and all ARs combined. Panels (a–f) show results for the cold season, and panels (g–m) for the warm season. The numbers in the upper left of each panel are the number of AR trajectories in each cluster, with the number in parentheses showing the percentage of AR trajectories within each cluster for the respective season. The numbers in the upper right show the fraction of moisture contributed by each cluster to the total AR-associated IWV for the respective season. The magenta lines represent the average trajectory of each cluster. Stippled areas indicate significant differences at the 0.05 level based on bootstrapping (see Text S1 for an explanation of the bootstrapping method). Regions where the magnitude of the values is less than 0.5% have been masked out. None of the differences for the Southern Hemisphere land and ocean are statistically significant, and thus are not shown.

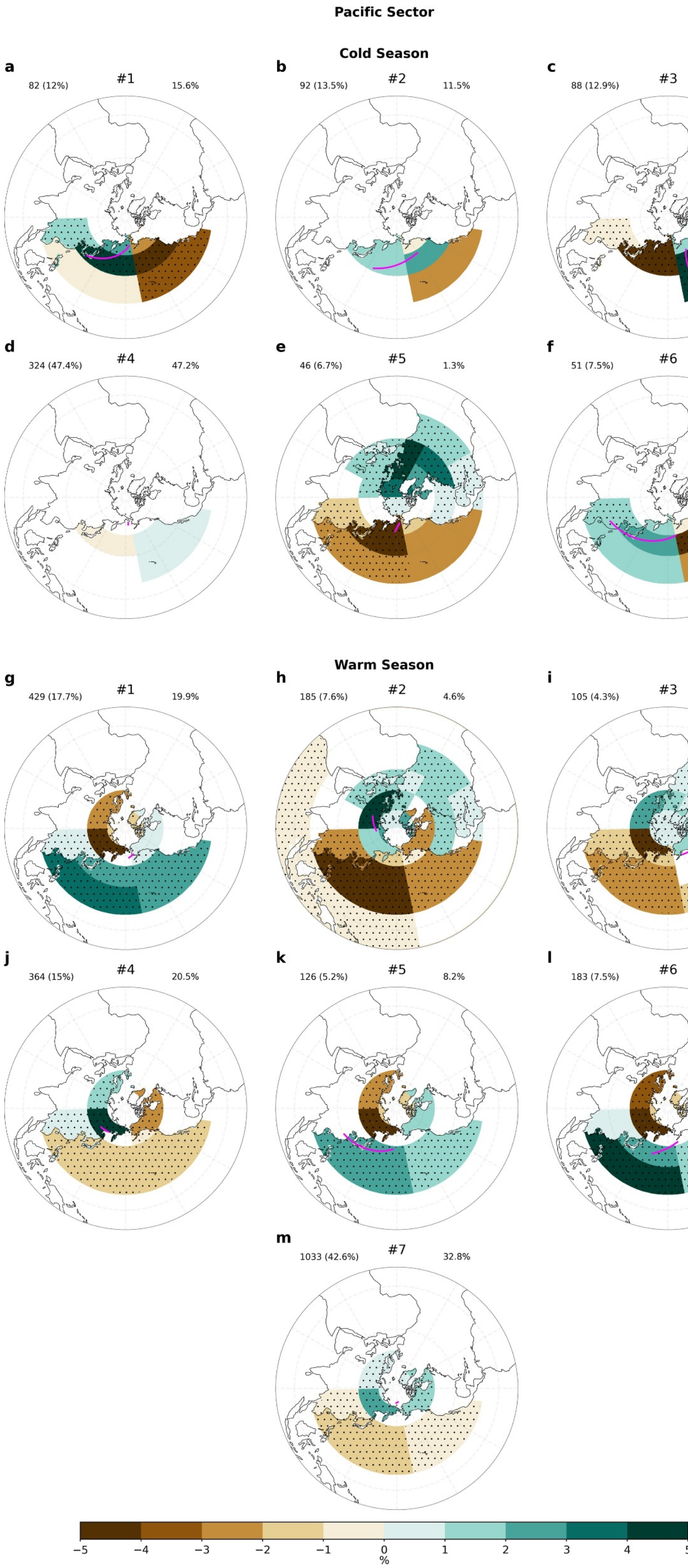

Figure 8. Same as Figure 7, but for the Pacific sector. Only the difference for the Southern Hemisphere ocean in (h), with a value of −0.62%, is statistically significant.

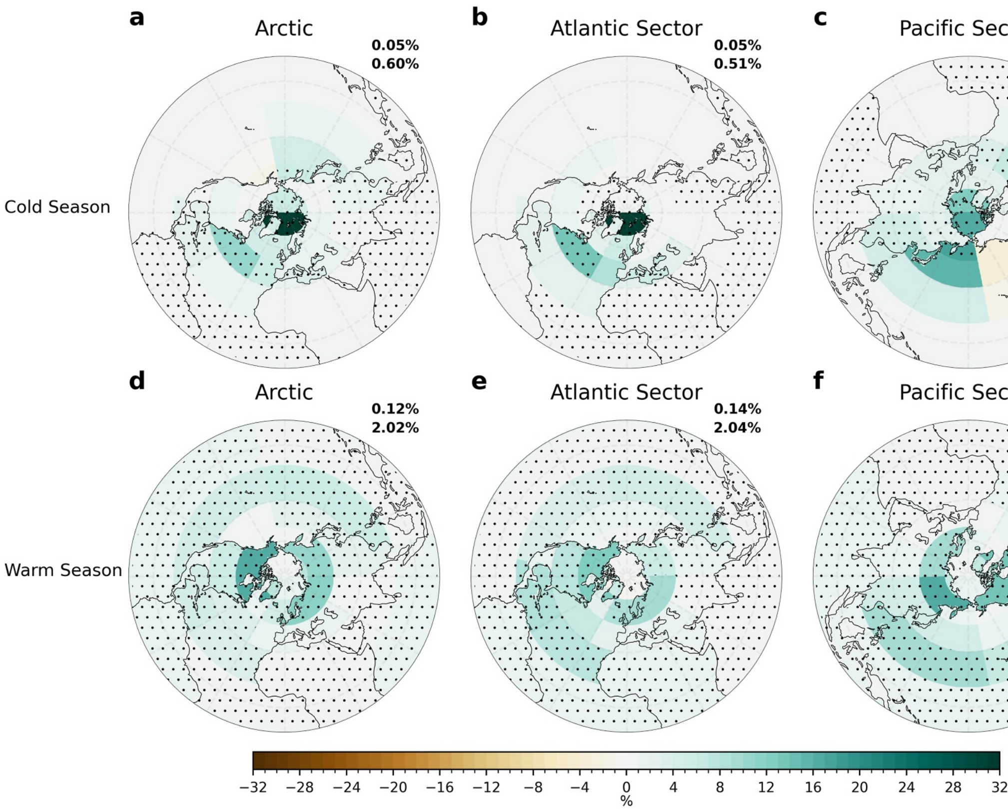

Figure 9. Fractional contribution from each source region to the mean integrated water vapor (IWV) trends in the Arctic (a, d), Atlantic sector (b, e), and Pacific sector (c, f). The top row is for the cold season, and the bottom row is for the warm season. Stippled areas indicate significant trends at the 0.05 level based on the Student's *t*-test. The values in the upper right of each panel indicate the fractional contributions from Southern Hemisphere land (top value) and ocean (bottom value). Bolded values indicate statistically significant differences at the 0.05 level.

season Arctic moistening in recent decades is strongly driven by an increase in locally sourced moisture, contributing 46.2%, with the Eastern Arctic alone accounting for 35.8%. Contributions from external sources are dominated by the North Atlantic poleward of 10°N, which contributes 29.0%. Similar results are observed for the Atlantic sector (Figure 9b), where Arctic-sourced moisture contributes 47.2% to the cold-season moistening trend, with the Eastern Arctic Ocean alone contributing 43.9%. Among the external sources, the North Atlantic Ocean remains the most important source, contributing 34.8%. For the Pacific sector (Figure 9c), locally sourced moisture from the Arctic plays a smaller role, contributing 32.5% to the trend. However, the contribution from the Western Arctic Ocean increases, accounting for 16.8%. The North Atlantic continues to act as an important external source, contributing 17% to the Pacific sector moistening trend. Among the external sources, the North Pacific poleward of 10°N is the largest contributor, accounting for 29.5% of the trend. Notably, fractional contributions from the North Pacific exhibit a dipole pattern, with enhanced contributions from the western basin and reduced contributions from the eastern basin. This dipole pattern is likely driven by the weakening trend of the Aleutian Low, which creates a clockwise circulation anomaly over the North Pacific, enhancing moisture transport into the Arctic through the western basin while reducing it through the eastern basin (not shown). Interestingly, the Southern Hemisphere also contributes significantly to Arctic moistening. As shown in Figure S4 in Supporting Information S1, such a cross-equator transport likely contributes to moistening in the upper troposphere and/or stratosphere.

Contrary to the cold season, the warm-season Arctic moistening trend is dominated by increased contributions from external sources (Figure 9d), which account for 90.7% of the trend. Among these external sources, the mid- and high-latitude continents make up the largest fraction, contributing 48.6% to the trend. Similar patterns are observed in the Atlantic and Pacific sector trends (Figures 9e and 9f), with external sources contributing 95.6% and 92.0%, respectively. The mid- and high-latitude continents again serve as the most important external sources, contributing 38.1% and 49% to the moistening trends in the Atlantic and Pacific sectors, respectively. The

10.1029/2025JD043918

relatively minor contributions from local sources are likely in part due to the equatorward meridional wind trends over both the Atlantic and Pacific sectors (Figure S13d in Supporting Information S1), which export moisture originating from the Eastern and Western Arctic Oceans, causing moistening in lower-latitude regions (Figures S13a and S13b in Supporting Information S1). Consequently, the local contribution is dominated by moisture from Arctic land areas (Figure S13c in Supporting Information S1). For all three receptor regions, remote external sources from south of 30°N contribute significantly to the moistening trends, accounting for 27.4%, 32.7%, and 31.2% of the trends in the Arctic, Atlantic, and Pacific sectors, respectively. These increases in contributions from remote sources are likely due to the longer residence time of moisture in the warm season, allowing for longer-distance transport.

3.3.2. Source Attribution for the Trends in the Moisture Content of Extreme Transport Events

We next investigate the fractional contributions to the trends in the moisture content of extreme transport events. Specifically, for each year and season, we compute the 6-hourly average meridional moisture flux at 70°N separately for the Atlantic and Pacific sectors by averaging meridional IVT over the longitude ranges 20°W–40°E and 150°E−150°W, respectively. For each sector and season, the 99th percentile of the meridional IVT distribution is then calculated. Time steps exceeding this seasonal, sector-specific threshold are classified as extreme transport events, ensuring a consistent number of events is identified for each season and year. Our analysis shows that extreme transport events over the Atlantic sector have experienced significant moistening trends in recent decades for both seasons. However, in the Pacific sector, only the warm-season trend is significant. Unlike the mean moistening trends (Figure 9b), the cold-season moistening trend for extreme transport events over the Atlantic sector is primarily driven by external sources, particularly the North Atlantic, Mediterranean Sea, and western Europe, which contribute 54.2%, 15.6%, and 10.5%, respectively, to the total trend. Locally, Arctic-sourced moisture accounts for only 7.8% (Figure 10a). The warm-season trend for extreme transport events is similarly dominated by external sources (Figure 10b). The North Atlantic and western Europe remain key contributors, accounting for 71.5% and 14.0% of the trend, respectively. Additionally, remote sources from the equatorial eastern Pacific, equatorial Atlantic, and Southern Hemisphere oceans contribute significantly to the moistening trend associated with the extreme transport events. However, unlike its substantial contribution to climatological moisture, northern North America appears to contribute negatively to the moisture trend in warm-season extreme transport events. Further analysis is needed to understand the drivers of this negative contribution.

For extreme transport events in the Pacific sector, the insignificant moisture trend is likely related to the dipole pattern in fractional contributions over the North Pacific, which shows an enhancement of moisture sourced from the western North Pacific but a reduced contribution from the eastern North Pacific (Figure 10c). This dipole pattern is also likely driven by the weakening of the Aleutian Low, which produces a similar dipole pattern in the mean moisture trend (Figure 9c). Consistent with this spatial distribution, AR trend pattern over the North Pacific shows increases over the northwest Pacific and decreases over the southeast Pacific (not shown). The warm-season trend is predominantly driven by external sources, originating from the North Pacific and East Eurasia that account for 35.7% and 38.2% of the total trend, respectively.

4. Conclusions and Discussions

Atmospheric poleward moisture transport has long been recognized as an important mechanism driving Arctic Amplification (AA; Gong et al., 2017; Graversen & Burtu, 2016; Lee et al., 2017). Given that a large fraction of this transport is delivered by Arctic ARs, identifying where these ARs source their moisture is essential to understanding their changes and impact on AA. In this study, using the CAM5 model equipped with moisture-tagging and circulation-nudging capabilities, we performed a comprehensive source attribution for ARs entering the Arctic through both the Atlantic and Pacific sectors during 1980–2021. Compared to the climatological Arctic moisture, ARs tend to draw more moisture from remote oceanic regions during the cold season and from both remote oceanic and continental regions during the warm season (Figure 4). For ARs affecting the Atlantic sector, locally sourced moisture from the Eastern Arctic Ocean contributes only 7.4% and 2.9% of AR moisture in the cold and warm seasons, respectively. In both seasons, the North Atlantic serves as a key source region, contributing 73.2% and 41.3% of AR moisture in the cold and warm seasons, respectively. For ARs entering the Pacific sector, local sources play an even smaller role, with moisture from the Western Arctic Ocean accounting for only 0.9% and 1.9% of AR moisture in the cold and warm seasons, respectively. In contrast, the North Pacific is a major source, contributing 85.3% and 29.4% of AR moisture in the cold and warm seasons,

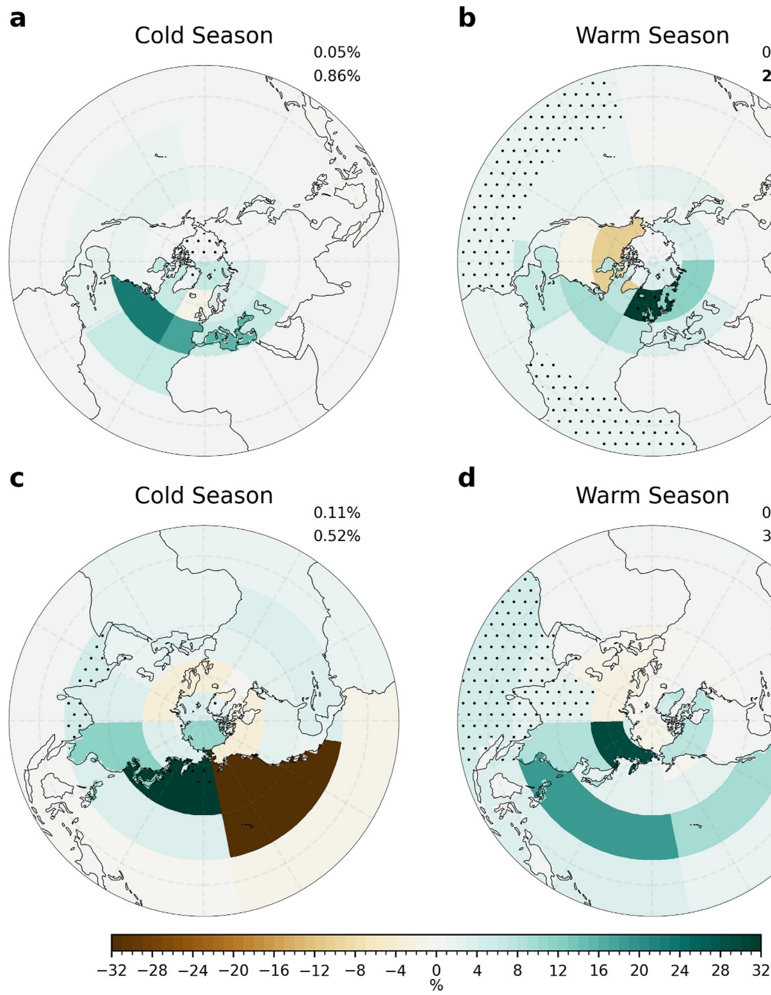

Figure 10. Same as Figure 9, but for the integrated water vapor (IWV) trends associated with extreme moisture transport events in the Atlantic sector (a, b) and the Pacific sector (c, d). The values in the upper right of each panel indicate the fractional contributions from Southern Hemisphere land (top value) and ocean (bottom value). Bolded values indicate statistically significant differences at the 0.05 level.

respectively. During the warm season, mid- and high-latitude continents are also significant sources, accounting for 40.1% and 51.3% of AR moisture for the Atlantic and Pacific sectors, respectively. The source attribution of Arctic ARs also exhibits intensity dependency, with stronger ARs drawing more moisture from remote oceanic regions (Figures 5 and 6). By examining the source regions of AR moisture at different altitudes, our results further confirm that AR moisture follows an ascending pathway as it flows poleward from more remote regions (Figure S7 in Supporting Information S1).

Previous studies on mid-latitude ARs have emphasized the importance of moisture convergence along their pathways (Bao et al., 2006; Dacre et al., 2015). Using a trajectory clustering technique, we demonstrate that Arctic ARs source moisture from both their genesis locations and pathways (Figures 7 and 8), with even small amounts of subtropical moisture being retained during the cold season. Lastly, the simulation configuration with prescribed SSTs and sea ice and circulation nudging, based on observational data, is ideal for trend analyses. The Arctic has been experiencing a moistening trend in both cold and warm seasons. Our results reveal that local and external sources play comparable roles in driving the cold-season moisture trend, with 46.2% of the contribution coming from local Arctic sources (Figure 9). In contrast, the warm-season moistening is predominantly driven by external sources, contributing 90.7%, particularly from high-latitude continents. Additionally, extreme transport events are also experiencing significant moistening trends, except for those over the Pacific sector during the cold season

(Figure 10). These moistening trends in extreme transport events are primarily driven by increased contributions from external sources.

The trajectory clustering technique used in this study allows us to demonstrate how the spatial distribution of source attribution depends on AR trajectories. This clustering technique has been widely applied in studies of tropical and extratropical cyclones (Camargo et al., 2007a; Gaffney et al., 2007; Mei & Xie, 2016). However, its application to ARs has been very limited. By employing this technique, Li et al. (2023) conducted a detailed study of cold-season North Atlantic ARs. In this study, we focus on the moisture uptake anomalies associated with each cluster of Arctic ARs. To enhance our understanding of Arctic ARs, further studies are needed to characterize the properties of each cluster, including their intensity, duration, and impacts on Arctic systems. Similar to Li et al. (2023), it would also be valuable to examine which climate modes drive their variability across different timescales to improve the predictability of Arctic ARs.

Previous studies have found that the amplified Arctic cold-season warming in recent decades is primarily driven by enhanced downward longwave radiation, which is largely caused by the moistening of the Arctic atmosphere due to increased poleward moisture flux from intraseasonal moisture intrusions (Gong et al., 2017; Lee et al., 2017). However, based on our trend analyses in Section 3.3, both local and external moisture sources play a comparable role in driving cold-season Arctic moistening. Our findings therefore appear to contradict previous studies that emphasize the dominant role of external moisture sources. One possible explanation for this discrepancy is that our model may overestimate the contribution of external sources to cold-season Arctic moistening. Alternatively, it is also plausible that, in addition to directly moistening the Arctic atmosphere through moisture transport, ARs may contribute indirectly. Arctic ARs are highly effective at inducing warming events and causing extreme sea ice loss (Ma, Wang, Chen, Qian, et al., 2024; Papritz et al., 2022; C. Zhang et al., 2023; P. Zhang et al., 2023). The melting of sea ice and the subsequent exposure of the underlying ocean by ARs can enhance local evaporation, thereby increasing the contribution of local moisture to cold-season Arctic moistening in recent decades. In either case, further studies are necessary to clarify the roles of Arctic ARs in the cold-season Arctic warming observed in recent decades.

Climate models exhibit significant biases in simulating the hydrological cycle (Abdelmoaty et al., 2021; Christopoulos & Schneider, 2021; Liu et al., 2014). As shown in this study, the CESM model employed for our study suffers from a moist bias in the mean state and simulates an overly strong warm-season moistening trend in the Arctic (Figures S1 and S12 in Supporting Information S1), even though the model is driven by observed SST and sea ice and constrained toward observed circulation with nudging. While uncovering the sources of these model biases is beyond the scope of our study, such model biases could pose a negative impact on the source attribution results. To improve the robustness of the results presented here, future research would benefit from similar studies using different climate models equipped with similar moisture-tagging capabilities, such as the Energy Exascale Earth System Model (E3SM) currently being developed (Nicole Feldl, personal communication). Additionally, beyond moisture-tagging simulations, Lagrangian methods using back trajectories could further enhance our understanding of event-based uncertainties in Arctic AR moisture source attribution associated with methodology.

In addition to model biases, another potential source of uncertainty arises from the choice of AR detection algorithm. As demonstrated in Ma, Wang, Chen, Leung, et al. (2024); see their Figures S5 and S6 in Supporting Information S1), the algorithms participating in the ARTMIP show substantial differences in their ability to capture Arctic ARs, with some detecting annual Arctic AR frequencies exceeding 10%, while others identify frequencies close to zero. This large spread highlights the sensitivity of Arctic AR detection to the specific criteria used by each algorithm. In this study, we find that stronger ARs tend to draw moisture from more remote regions. Therefore, algorithms that apply more restrictive criteria, identifying fewer but stronger ARs (Ralph et al., 2019; Rutz et al., 2019), are likely to emphasize moisture contributions from distant sources. Moreover, while the algorithm employed in this study considers both zonal and meridional components of IVT, some polar-specific algorithms (e.g., Wille et al., 2021) rely solely on meridional IVT, thereby placing greater emphasis on meridional moisture transport. As a result, applying such algorithms may shift the inferred importance of remote source regions. Given the increasing number of detection algorithms now available, a comprehensive intercomparison among multiple algorithms over the polar regions would be a valuable direction for future research. Such efforts could help quantify the methodological uncertainty and strengthen confidence in the source attribution of Arctic

AR moisture. Nevertheless, the results and methodologies presented in this study represent an important step toward a better understanding of both the Arctic hydrological cycle and Arctic AR moisture sources.

A previous study found that North Pacific ARs may source moisture from even more remote regions under a warmer climate (Nusbaumer & Noone, 2018). It remains unclear whether similar responses also exist in Arctic ARs. As the spatial pattern of future warming has shown to be highly heterogeneous, the findings of this study under the current climate have significant implications for future changes in Arctic ARs.

Conflict of Interest

The authors declare no conflicts of interest relevant to this study.

Data Availability Statement

The AR detection algorithm can be downloaded at https://doi.org/10.25346/S6/B89KXF. The trajectory clustering algorithm can be accessed at http://www.datalab.uci.edu/resources/CCT/. Model output from the moisture-tagging simulation will be made available upon request. ERA5 can be found at: https://cds.climate.copernicus.eu/datasets/reanalysis-era5-pressure-levels?tab=download.The CAM5 documentation can be accessed through: https://ncar.github.io/CAM_SciDoc/doc/build/html/cam5_scientific_guide/index.html.

Acknowledgments

This research was supported by the U.S. Department of Energy (DOE), Office of Science, Office of Biological and Environmental Research, Regional and Global Model Analysis program area. This research used resources of the National Energy Research Scientific Computing Center (NERSC), a U.S. DOE Office of Science User Facility operated under Contract No. DE-AC02-05CH11231, as part of NERSC award m1199. The Pacific Northwest National Laboratory (PNNL) is operated for DOE by Battelle Memorial Institute under contract DE-AC05-76RLO1830. NF and AA were supported under DOE Award Number DE-SC0023070.

References

Abdelmoaty, H. M., Papalexiou, S. M., Rajulapati, C. R., & AghaKouchak, A. (2021). Biases beyond the mean in CMIP6 extreme precipitation: A global investigation. *Earth's Future*, *9*(10), e2021EF002196. https://doi.org/10.1029/2021ef002196

Amstrup, S. C., DeWeaver, E. T., Douglas, D. C., Marcot, B. G., Durner, G. M., Bitz, C. M., & Bailey, D. A. (2010). Greenhouse gas mitigation can reduce sea-ice loss and increase polar bear persistence. *Nature*, *468*(7326), 955–958. https://doi.org/10.1038/nature09653

Årthun, M., Onarheim, I. H., Dörr, J., & Eldevik, T. (2021). The seasonal and regional transition to an ice-free Arctic. *Geophysical Research Letters*, *48*(1), e2020GL090825. https://doi.org/10.1029/2020gl090825

Bao, J. W., Michelson, S. A., Neiman, P. J., Ralph, F. M., & Wilczak, J. M. (2006). Interpretation of enhanced integrated water vapor bands associated with extratropical cyclones: Their formation and connection to tropical moisture. *Monthly Weather Review*, *134*(4), 1063–1080. https://doi.org/10.1175/mwr3123.1

Bosilovich, M. G., Sud, Y. C., Schubert, S. D., & Walker, G. K. (2003). Numerical simulation of the large-scale North American monsoon water sources. *Journal of Geophysical Research*, *108*(D16). https://doi.org/10.1029/2002jd003095

Camargo, S. J., Robertson, A. W., Gaffney, S. J., Smyth, P., & Ghil, M. (2007a). Cluster analysis of typhoon tracks. Part I: General properties. *Journal of Climate*, *20*(14), 3635–3653. https://doi.org/10.1175/jcli4188.1

Camargo, S. J., Robertson, A. W., Gaffney, S. J., Smyth, P., & Ghil, M. (2007b). Cluster analysis of typhoon tracks. Part II: Large-scale circulation and ENSO. *Journal of Climate*, *20*(14), 3654–3676. https://doi.org/10.1175/jcli4203.1

Christopoulos, C., & Schneider, T. (2021). Assessing biases and climate implications of the diurnal precipitation cycle in climate models. *Geophysical Research Letters*, *48*(13), e2021GL093017. https://doi.org/10.1029/2021gl093017

Chylek, P., Folland, C., Klett, J. D., Wang, M., Hengartner, N., Lesins, G., & Dubey, M. K. (2022). Annual mean Arctic amplification 1970--2020: Observed and simulated by CMIP6 climate models. *Geophysical Research Letters*, *49*(13), e2022GL099371. https://doi.org/10.1029/2022gl099371

Cordeira, J. M., Stock, J., Dettinger, M. D., Young, A. M., Kalansky, J. F., & Ralph, F. M. (2019). A 142-year climatology of northern California landslides and atmospheric rivers. *Bulletin of the American Meteorological Society*, *100*(8), 1499–1509. https://doi.org/10.1175/bams-d-18-0158.1

Corringham, T. W., Ralph, F. M., Gershunov, A., Cayan, D. R., & Talbot, C. A. (2019). Atmospheric rivers drive flood damages in the western United States. *Science Advances*, *5*(12), eaax4631. https://doi.org/10.1126/sciadv.aax4631

Curry, J. A., Schramm, J. L., Rossow, W. B., & Randall, D. (1996). Overview of Arctic cloud and radiation characteristics. *Journal of Climate*, *9*(8), 1731–1764. https://doi.org/10.1175/1520-0442(1996)009<1731:ooacar>2.0.co;2

Dacre, H. F., Clark, P. A., Martinez-Alvarado, O., Stringer, M. A., & Lavers, D. A. (2015). How do atmospheric rivers form? *Bulletin of the American Meteorological Society*, *96*(8), 1243–1255. https://doi.org/10.1175/bams-d-14-00031.1

Dettinger, M. D., Ralph, F. M., Das, T., Neiman, P. J., & Cayan, D. R. (2011). Atmospheric rivers, floods and the water resources of California. *Water*, *3*(2), 445–478. https://doi.org/10.3390/w3020445

Dufour, A., Zolina, O., & Gulev, S. K. (2016). Atmospheric moisture transport to the Arctic: Assessment of reanalyses and analysis of transport components. *Journal of Climate*, *29*(14), 5061–5081. https://doi.org/10.1175/jcli-d-15-0559.1

Eiras-Barca, J., Dominguez, F., Hu, H., Garaboa-Paz, D., & Miguez-Macho, G. (2017). Evaluation of the moisture sources in two extreme landfalling atmospheric river events using an Eulerian WRF tracers tool. *Earth System Dynamics*, *8*(4), 1247–1261. https://doi.org/10.5194/esd-8-1247-2017

Ford, J. D., Pearce, T., Canosa, I. V., & Harper, S. (2021). The rapidly changing Arctic and its societal implications. *Wiley Interdisciplinary Reviews: Climate Change*, *12*(6), e735. https://doi.org/10.1002/wcc.735

Gaffney, S. J., Robertson, A. W., Smyth, P., Camargo, S. J., & Ghil, M. (2007). Probabilistic clustering of extratropical cyclones using regression mixture models [Software]. *Climate Dynamics*, *29*(4), 423–440. https://doi.org/10.1007/s00382-007-0235-z

Gimeno, L., Stohl, A., Trigo, R. M., Dominguez, F., Yoshimura, K., Yu, L., et al. (2012). Oceanic and terrestrial sources of continental precipitation. *Reviews of Geophysics*, *50*(4), RG4003. https://doi.org/10.1029/2012RG000389

Gimeno, L., Vázquez, M., Eiras-Barca, J., Sori, R., Algarra, I., & Nieto, R. (2019). Atmospheric moisture transport and the decline in Arctic Sea ice. *Wiley Interdisciplinary Reviews: Climate Change*, *10*(4), e588.

Gong, T., Feldstein, S., & Lee, S. (2017). The role of downward infrared radiation in the recent Arctic winter warming trend. *Journal of Climate*, *30*(13), 4937–4949. https://doi.org/10.1175/jcli-d-16-0180.1

Graversen, R. G., & Burtu, M. (2016). Arctic amplification enhanced by latent energy transport of atmospheric planetary waves. *Quarterly Journal of the Royal Meteorological Society*, *142*(698), 2046–2054. https://doi.org/10.1002/qj.2802

Guan, B., & Waliser, D. E. (2015). Detection of atmospheric rivers: Evaluation and application of an algorithm for global studies. *Journal of Geophysical Research: Atmospheres*, *120*(24), 12514–12535. https://doi.org/10.1002/2015jd024257

Guan, B., & Waliser, D. E. (2019). Tracking atmospheric rivers globally: Spatial distributions and temporal evolution of life cycle characteristics [Software]. *Journal of Geophysical Research: Atmospheres*, *124*(23), 12523–12552. https://doi.org/10.1029/2019JD031205

Hegyi, B. M., & Taylor, P. C. (2018). The unprecedented 2016–2017 Arctic Sea ice growth season: The crucial role of atmospheric rivers and longwave fluxes. *Geophysical Research Letters*, *45*(10), 5204–5212. https://doi.org/10.1029/2017GL076717

Hersbach, H., Bell, B., Berrisford, P., Hirahara, S., Horányi, A., Muñoz-Sabater, J., et al. (2020). The ERA5 global reanalysis [Dataset]. *Quarterly Journal of the Royal Meteorological Society*, *146*(730), 1999–2049. https://doi.org/10.1002/qj.3803

Hu, H., & Dominguez, F. (2019). Understanding the role of tropical moisture in atmospheric rivers. *Journal of Geophysical Research: Atmospheres*, *124*(24), 13826–13842. https://doi.org/10.1029/2019JD030867

Huang, B., Thorne, P. W., Banzon, V. F., Boyer, T., Chepurin, G., Lawrimore, J. H., et al. (2017). Extended reconstructed sea surface temperature, version 5 (ERSSTv5): Upgrades, validations, and intercomparisons. *Journal of Climate*, *30*(20), 8179–8205. https://doi.org/10.1175/jcli-d-16-0836.1

Hurrell, J. W., Holland, M. M., Gent, P. R., Ghan, S., Kay, J. E., Kushner, P. J., et al. (2013). The Community Earth System Model: A framework for collaborative research. *Bulletin of the American Meteorological Society*, *94*(9), 1339–1360. https://doi.org/10.1175/bams-d-12-00121.1

Jahn, A., Holland, M. M., & Kay, J. E. (2024). Projections of an ice-free Arctic Ocean. *Nature Reviews Earth \& Environment*, *5*(3), 164–176. https://doi.org/10.1038/s43017-023-00515-9

Jiang, J., Zhou, T., Wang, H., Qian, Y., Noone, D., & Man, W. (2020). Tracking moisture sources of precipitation over central Asia: A study based on the water-source-tagging method. *Journal of Climate*, *33*(23), 10339–10355. https://doi.org/10.1175/jcli-d-20-0169.1

Lavers, D. A., & Villarini, G. (2013). The nexus between atmospheric rivers and extreme precipitation across Europe. *Geophysical Research Letters*, *40*(12), 3259–3264. https://doi.org/10.1002/grl.50636

Lavers, D. A., & Villarini, G. (2015). The contribution of atmospheric rivers to precipitation in Europe and the United States. *Journal of Hydrology*, *522*, 382–390. https://doi.org/10.1016/j.jhydrol.2014.12.010

Lee, S., Gong, T., Feldstein, S. B., Screen, J. A., & Simmonds, I. (2017). Revisiting the cause of the 1989--2009 Arctic surface warming using the surface energy budget: Downward infrared radiation dominates the surface fluxes. *Geophysical Research Letters*, *44*(20), 10–654. https://doi.org/10.1002/2017gl075375

Leung, L. R., & Qian, Y. (2009). Atmospheric rivers induced heavy precipitation and flooding in the western U.S. simulated by the WRF regional climate model. *Geophysical Research Letters*, *36*(3), 1–6. https://doi.org/10.1029/2008GL036445

Li, C., Mei, W., & Kamae, Y. (2023). A cluster analysis of cold-season atmospheric river tracks over the North Atlantic and their linkages to extreme precipitation and winds. *Climate Dynamics*, *60*(1), 201–212. https://doi.org/10.1007/s00382-022-06297-y

Li, L., Cannon, F., Mazloff, M. R., Subramanian, A. C., Wilson, A. M., & Ralph, F. M. (2024). Impact of atmospheric rivers on Arctic sea ice variations. *The Cryosphere*, *18*(1), 121–137. https://doi.org/10.5194/tc-18-121-2024

Liu, C., & Barnes, E. A. (2015). Extreme moisture transport into the Arctic linked to Rossby wave breaking. *Journal of Geophysical Research: Atmospheres*, *120*(9), 3774–3788. https://doi.org/10.1002/2014jd022796

Liu, Z., Mehran, A., Phillips, T. J., & AghaKouchak, A. (2014). Seasonal and regional biases in CMIP5 precipitation simulations. *Climate Research*, *60*(1), 35–50. https://doi.org/10.3354/cr01221

Luo, B., Luo, D., Wu, L., Zhong, L., & Simmonds, I. (2017). Atmospheric circulation patterns which promote winter Arctic sea ice decline. *Environmental Research Letters*, *12*(5), 054017. https://doi.org/10.1088/1748-9326/aa69d0

Ma, W., & Chen, G. (2022). What controls the interannual variability of the Boreal winter atmospheric river activities over the Northern Hemisphere? *Journal of Climate*, *35*(23), 7555–7573. https://doi.org/10.1175/jcli-d-22-0089.1

Ma, W., Chen, G., & Guan, B. (2020). Poleward shift of atmospheric rivers in the Southern Hemisphere in recent decades. *Geophysical Research Letters*, *47*(21), 1–11. https://doi.org/10.1029/2020GL089934

Ma, W., Chen, G., Peings, Y., & Alviz, N. (2021). Atmospheric river response to Arctic Sea ice loss in the polar amplification model intercomparison project. *Geophysical Research Letters*, *48*(20), 1–12. https://doi.org/10.1029/2021gl094883

Ma, W., Norris, J., & Chen, G. (2020). Projected changes to extreme precipitation along North American West coast from the CESM large ensemble. *Geophysical Research Letters*, *47*(1), 1–10. https://doi.org/10.1029/2019GL086038

Ma, W., Wang, H., Chen, G., Leung, L. R., Lu, J., Rasch, P. J., et al. (2024). The role of interdecadal climate oscillations in driving Arctic atmospheric river trends. *Nature Communications*, *15*(1), 2135. https://doi.org/10.1038/s41467-024-45159-5

Ma, W., Wang, H., Chen, G., Qian, Y., Baxter, I., Huo, Y., & Seefeldt, M. W. (2024). Wintertime extreme warming events in the high Arctic: Characteristics, drivers, trends, and the role of atmospheric rivers. *Atmospheric Chemistry and Physics*, *24*(7), 4451–4472. https://doi.org/10.5194/acp-24-4451-2024

Mattingly, K. S., Mote, T. L., & Fettweis, X. (2018). Atmospheric river impacts on Greenland Ice Sheet surface mass balance. *Journal of Geophysical Research: Atmospheres*, *123*(16), 8538–8560. https://doi.org/10.1029/2018jd028714

Mei, W., & Xie, S. P. (2016). Intensification of landfalling typhoons over the northwest Pacific since the late 1970s. *Nature Geoscience*, *9*(10), 753–757. https://doi.org/10.1038/ngeo2792

Meier, W. N., Hovelsrud, G. K., Oort, B. E. H., Key, J. R., Kovacs, K. M., Michel, C., et al. (2014). Arctic sea ice in transformation: A review of recent observed changes and impacts on biology and human activity. *Reviews of Geophysics*, *51*, 185–217. https://doi.org/10.1002/2013RG000431.Received

Murto, S., Caballero, R., Svensson, G., & Papritz, L. (2022). Interaction between Atlantic cyclones and Eurasian atmospheric blocking drives wintertime warm extremes in the high Arctic. *Weather and Climate Dynamics*, *3*(1), 21–44. https://doi.org/10.5194/wcd-3-21-2022

NASA. (2021). Arctic Sea ice minimum extent | vital signs—Climate change: Vital signs of the planet. Retrieved from https://climate.nasa.gov/vital-signs/arctic-sea-ice/?intent=121

Neale, R. B., Chen, C.-C., Gettelman, A., Lauritzen, P. H., Park, S., Williamson, D. L., et al. (2010). Description of the NCAR community atmosphere model (CAM 5.0). NCAR Tech. Note Ncar/Tn-486+ STR (Vol. *1*, pp. 1–12).

Nusbaumer, J., & Noone, D. (2018). Numerical evaluation of the modern and future origins of atmospheric river moisture over the west coast of the United States. *Journal of Geophysical Research: Atmospheres*, *123*(12), 6423–6442. https://doi.org/10.1029/2017JD028081

Nusbaumer, J., Wong, T. E., Bardeen, C., & Noone, D. (2017). Evaluating hydrological processes in the Community Atmosphere Model Version 5 (C AM5) using stable isotope ratios of water. *Journal of Advances in Modeling Earth Systems*, *9*(2), 949–977. https://doi.org/10.1002/2016ms000839

Oleson, K. W. (2010). *Technical description of version 4.0 of the Community Land Model (CLM)* (Vol. 257). NCAR Technical Note.

Pan, C., Zhu, B., Gao, J., & Kang, H. (2017). Source apportionment of atmospheric water over East Asia--a source tracer study in CAM5. 1. *Geoscientific Model Development*, *10*(2), 673–688. https://doi.org/10.5194/gmd-10-673-2017

Papritz, L., Hauswirth, D., & Hartmuth, K. (2022). Moisture origin, transport pathways, and driving processes of intense wintertime moisture transport into the Arctic. *Weather and Climate Dynamics*, *3*(1), 1–20. https://doi.org/10.5194/wcd-3-1-2022

Payne, A. E., Demory, M.-E., Leung, L. R., Ramos, A. M., Shields, C. A., Rutz, J. J., et al. (2020). Responses and impacts of atmospheric rivers to climate change. *Nature Reviews Earth & Environment*, *1*(3), 143–157. https://doi.org/10.1038/s43017-020-0030-5

Post, E., Bhatt, U. S., Bitz, C. M., Brodie, J. F., Fulton, T. L., Hebblewhite, M., et al. (2013). Ecological consequences of sea-ice decline. *Science*, *341*(6145), 519–524. https://doi.org/10.1126/science.1235225

Ralph, F. M., Neiman, P. J., Wick, G. A., Gutman, S. I., Dettinger, M. D., Cayan, D. R., & White, A. B. (2006). Flooding on California's Russian River: Role of atmospheric rivers. *Geophysical Research Letters*, *33*(13), L13801. https://doi.org/10.1029/2006GL026689

Ralph, F. M., Wilson, A. M., Shulgina, T., Kawzenuk, B., Sellars, S., Rutz, J. J., et al. (2019). ARTMIP-early start comparison of atmospheric river detection tools: How many atmospheric rivers hit northern California's Russian River watershed? *Climate Dynamics*, *52*(7–8), 4973–4994. https://doi.org/10.1007/s00382-018-4427-5

Rantanen, M., Karpechko, A. Y., Lipponen, A., Nordling, K., Hyvärinen, O., Ruosteenoja, K., et al. (2022). The Arctic has warmed nearly four times faster than the globe since 1979. *Communications Earth & Environment*, *3*(1), 168. https://doi.org/10.1038/s43247-022-00498-3

Rutllant, J. A., Matus, F., Rudloff, V., & Rondanelli, R. (2023). The role of atmospheric rivers in rainfall-induced landslides: A study from the Elqui valley. *Journal of Arid Environments*, *216*, 105016. https://doi.org/10.1016/j.jaridenv.2023.105016

Rutz, J. J., Shields, C. A., Lora, J. M., Payne, A. E., Guan, B., Ullrich, P., et al. (2019). The atmospheric river tracking method intercomparison project (ARTMIP): Quantifying uncertainties in atmospheric river climatology. *Journal of Geophysical Research: Atmospheres*, *124*(24), 13777–13802. https://doi.org/10.1029/2019jd030936

Rutz, J. J., & Steenburgh, W. J. (2012). Quantifying the role of atmospheric rivers in the interior western United States. *Atmospheric Science Letters*, *13*(4), 257–261. https://doi.org/10.1002/asl.392

Serreze, M. C., Crawford, A. D., & Barrett, A. P. (2015). Extreme daily precipitation events at Spitsbergen, an Arctic Island. *International Journal of Climatology*, *35*(15), 4574–4588. https://doi.org/10.1002/joc.4308

Serreze, M. C., Voveris, J., Barrett, A. P., Fox, S., Blanken, P. D., & Crawford, A. (2022). Characteristics of extreme daily precipitation events over the Canadian Arctic. *International Journal of Climatology*, *42*(16), 10353–10372. https://doi.org/10.1002/joc.7907

Simpson, I. R., Bacmeister, J., Neale, R. B., Hannay, C., Gettelman, A., Garcia, R. R., et al. (2020). An evaluation of the large-scale atmospheric circulation and its variability in CESM2 and other CMIP models. *Journal of Geophysical Research: Atmospheres*, *125*(13), e2020JD032835. https://doi.org/10.1029/2020jd032835

Singh, H. A., Bitz, C. M., Nusbaumer, J., & Noone, D. C. (2016). A mathematical framework for analysis of water tracers: Part 1: Development of theory and application to the preindustrial mean state. *Journal of Advances in Modeling Earth Systems*, *8*(2), 991–1013. https://doi.org/10.1002/2016ms000649

Singh, H. K. A., Bitz, C. M., Donohoe, A., Nusbaumer, J., & Noone, D. C. (2016). A mathematical framework for analysis of water tracers. Part II: Understanding large-scale perturbations in the hydrological cycle due to CO_2 doubling. *Journal of Climate*, *29*(18), 6765–6782. https://doi.org/10.1175/jcli-d-16-0293.1

Singh, H. K. A., Bitz, C. M., Donohoe, A., & Rasch, P. J. (2017). A source--receptor perspective on the polar hydrologic cycle: Sources, seasonality, and Arctic--Antarctic parity in the hydrologic cycle response to CO_2 doubling. *Journal of Climate*, *30*(24), 9999–10017. https://doi.org/10.1175/jcli-d-16-0917.1

Sodemann, H., Schwierz, C., & Wernli, H. (2008). Interannual variability of Greenland winter precipitation sources: Lagrangian moisture diagnostic and North Atlantic Oscillation influence. *Journal of Geophysical Research*, *113*(D3). https://doi.org/10.1029/2007jd008503

Sodemann, H., & Stohl, A. (2013). Moisture origin and meridional transport in atmospheric rivers and their association with multiple cyclones. *Monthly Weather Review*, *141*(8), 2850–2868. https://doi.org/10.1175/MWR-D-12-00256.1

Sodemann, H., Wernli, H., & Schwierz, C. (2009). Sources of water vapour contributing to the Elbe flood in August 2002—A tagging study in a mesoscale model. *Quarterly Journal of the Royal Meteorological Society: A Journal of the Atmospheric Sciences, Applied Meteorology and Physical Oceanography*, *135*(638), 205–223. https://doi.org/10.1002/qj.374

Sweeney, A. J., Fu, Q., Po-Chedley, S., Wang, H., & Wang, M. (2023). Internal variability increased Arctic amplification during 1980--2022. *Geophysical Research Letters*, *50*(24), e2023GL106060. https://doi.org/10.1029/2023gl106060

Vázquez, M., Algarra, I., Eiras-Barca, J., Ramos, A. M., Nieto, R., & Gimeno, L. (2018). Atmospheric rivers over the Arctic: Lagrangian characterisation of their moisture sources. *Water*, *11*(1), 1–14. https://doi.org/10.3390/w11010041

Vázquez, M., Nieto, R., Drumond, A., & Gimeno, L. (2016). Moisture transport into the Arctic: Source-receptor relationships and the roles of atmospheric circulation and evaporation. *Journal of Geophysical Research*, *121*(22), 13493–13509. https://doi.org/10.1002/2016JD025400

von Deimling, T., Lee, H., Ingeman-Nielsen, T., Westermann, S., Romanovsky, V., Lamoureux, S., et al. (2021). Consequences of permafrost degradation for Arctic infrastructure--bridging the model gap between regional and engineering scales. *The Cryosphere*, *15*(5), 2451–2471. https://doi.org/10.5194/tc-15-2451-2021

Waliser, D., & Guan, B. (2017). Extreme winds and precipitation during landfall of atmospheric rivers. *Nature Geoscience*, *10*(3), 179–183. https://doi.org/10.1038/ngeo2894

Wang, H., Fyke, J. G., Lenaerts, J. T. M., Nusbaumer, J. M., Singh, H., Noone, D., et al. (2020). Influence of sea-ice anomalies on Antarctic precipitation using source attribution in the Community Earth System Model. *The Cryosphere*, *14*(2), 429–444. https://doi.org/10.5194/tc-14-429-2020

Wang, X., Liu, Y., Key, J. R., & Dworak, R. (2022). A new perspective on four decades of changes in arctic sea ice from satellite observations. *Remote Sensing*, *14*(8), 1846. https://doi.org/10.3390/rs14081846

Wille, J. D., Favier, V., Gorodetskaya, I. V., Agosta, C., Kittel, C., Beeman, J. C., et al. (2021). Antarctic atmospheric river climatology and precipitation impacts. *Journal of Geophysical Research: Atmospheres*, *126*(8), 1–20. https://doi.org/10.1029/2020JD033788

Woods, C., & Caballero, R. (2016). The role of moist intrusions in winter arctic warming and sea ice decline. *Journal of Climate*, *29*(12), 4473–4485. https://doi.org/10.1175/JCLI-D-15-0773.1

Woods, C., Caballero, R., & Svensson, G. (2013). Large-scale circulation associated with moisture intrusions into the Arctic during winter. *Geophysical Research Letters*, *40*(17), 4717–4721. https://doi.org/10.1002/grl.50912

Zhang, C., Tung, W. W., & Cleveland, W. S. (2023). Climatology and decadal changes of Arctic atmospheric rivers based on ERA5 and MERRA-2. *Environmental Research: Climate*, *2*(3), 035005. https://doi.org/10.1088/2752-5295/acdf0f

Zhang, P., Chen, G., Ting, M., Ruby Leung, L., Guan, B., & Li, L. (2023). More frequent atmospheric rivers slow the seasonal recovery of Arctic sea ice. *Nature Climate Change*, *13*(3), 266–273. https://doi.org/10.1038/s41558-023-01599-3

Zhang, R., Wang, H., Fu, Q., Rasch, P. J., Wu, M., & Maslowski, W. (2021). Understanding the cold season Arctic surface warming trend in recent decades. *Geophysical Research Letters*, *48*(19), e2021GL094878. https://doi.org/10.1029/2021gl094878

Zhang, S., Zhang, K., Wan, H., & Sun, J. (2022). Further improvement and evaluation of nudging in the E3SM Atmosphere Model version 1 (EAMv1): Simulations of the mean climate, weather events, and anthropogenic aerosol effects. *Geoscientific Model Development*, *15*(17), 6787–6816. https://doi.org/10.5194/gmd-15-6787-2022